Organic & Biomolecular Chemistry

Dynamic Article Links

Cite this: *Org. Biomol. Chem.*, 2012, **10**, 1285

www.rsc.org/obc

**PAPER**

# Trichogin GA IV: A versatile template for the synthesis of novel peptaibiotics†‡

**Marta De Zotti,[a] Barbara Biondi,[a] Cristina Peggion,[a] Fernando Formaggio,[a] Yoonkyung Park,[b,c] Kyung-Soo Hahm[b,d] and Claudio Toniolo*[a]**

***Received 15th July 2011, Accepted 8th November 2011***
**DOI: 10.1039/c1ob06178j**



Trichogin GA IV, isolated from the fungus *Trichoderma longibrachiatum*, is the prototype of lipopeptaibols, the sub-class of short-length peptaibiotics exhibiting membrane-modifying properties. This peptaibol is predominantly folded in a mixed $3_{10}$-/α- helical conformation with a clear, albeit modest, amphiphilic character, which is likely to be responsible for its capability to perturb bacterial membranes and to induce cell death. In previous papers, we reported on the interesting biological properties of trichogin GA IV, namely its good activity against Gram positive bacteria, in particular methicillin-resistant *S. aureus* strains, its stability towards proteolytic degradation, and its low hemolytic activity. Aiming at broadening the antimicrobial activity spectrum by increasing the peptide helical amphiphilicity, in this work we synthesized, by solution and solid-phase methodologies, purified and fully characterized a set of trichogin GA IV analogs in which the four Gly residues at positions 2, 5, 6, 9, lying in the poorly hydrophilic face of the helical structure, are substituted by one (position 2, 5, 6 or 9), two (positions 5 and 6), three (positions 2, 5, and 9), and four (positions 2, 5, 6, and 9) Lys residues. The conformational preferences of the Lys-containing analogs were assessed by FT-IR absorption, CD and 2D-NMR techniques in aqueous, organic, and membrane-mimetic environments. Interestingly, it turns out that the presence of charged residues induces a transition of the helical conformation adopted by the peptaibols (from $3_{10}$- to α-helix) as a function of pH in a reversible process. The role played in the analogs by the markedly increased amphiphilicity was further tested by fluorescence leakage experiments in model membranes, protease resistance, antibacterial and antifungal activities, cytotoxicity, and hemolysis. Taken together, our biological results provide evidence that some of the least substituted among these analogs are good candidates for the development of new membrane-active antimicrobial agents.

## Introduction

Conventional antibiotics target definite sites, such as specific enzymes or DNA, in bacteria. For this reason, microorganism resistance may occur with high probability. The clinical impact of antibiotic resistance implies high cost and mortality. Plant and animal kingdoms are rich sources of antimicrobial peptides (AMPs) physically disrupting bacterial cell membranes. This diverse mechanism of action makes them less susceptible to resistance.[1–3]

Among AMPs, there is a group of natural antibacterial peptides, the lipopeptaibols (short-length peptaibiotics[4]), characterized by an N-terminal long-chain fatty acid protecting group, high amount of the noncoded amino acid Aib (α-aminoisobutyric acid) and a C-terminal 1,2-amino alcohol. Most lipopeptaibols exhibit remarkably valuable properties, such as well developed helicity, amphiphilicity, stability to proteolytic degradation, and short main-chain length.[5] These properties render them intriguing lead compounds in the search of candidates as novel, potent antibacterial agents. Trichogin GA IV[6] is considered the prototype of lipopeptaibols. It was isolated in 1992 as the main component of the natural (*Trichoderma longibrachiatum*) trichogin microheterogeneous mixture and sequenced by Bodo and coworkers.[7,8] The 10-mer amino acid primary structure of trichogin GA IV is blocked at the N-terminus by an *n*-octanoyl (*n*-Oct) moiety and has a chiral (*S*) 1,2-aminoalcohol, Lol (leucinol), at the C-terminus. The sequence is as follows:

[a]*ICB, Padova Unit, CNR, Department of Chemistry, University of Padova, 35131, Padova, Italy. E-mail: claudio.toniolo@unipd.it; Fax: +39 049 8275829; Tel: +39 049 8275247*
[b]*Research Center for Proteinous Materials, Chosun University, Gwangju, 501-759, Korea*
[c]*Department of Biotechnology, Chosun University, Gwangju, 501-759, Korea*
[d]*Department of Cellular Molecular Medicine, School of Medicine, Chosun University, Gwangju, 501-759, Korea*

† Electronic supplementary information (ESI) available. See DOI: 10.1039/c1ob06178j

‡ This article is part of an *Organic & Biomolecular Chemistry* web theme issue on Foldamer Chemistry.

***n*-Oct-Aib-Gly-Leu-Aib-Gly-Gly-Leu-Aib-Gly-Ile-Lol**

On the basis of the results from a number of conformational investigations, including X-ray diffraction analyses, on synthetic trichogin GA IV and selected analogs, mostly carried out by some of us (C.P., F.F., and C.T.), a right-handed helical structure was suggested.[6,7,9–19] This conclusion is not surprising in view of the heavy presence (30%) of the strongly helicogenic Aib residues in the sequence.[20–23] It was also proposed that the flexible -Gly$^5$-Gly$^6$- dipeptide would create a hinge point between two helical regions. The overall mixed $3_{10}$-/α- helical structure[24,25] is largely amphiphilic, with the hydrophobic face including the *n*-Oct group and the Leu, Ile, and Lol side chains, while the opposite face is characterized by the four Gly residues strategically located at positions 2, 5, 6, and 9. In refs. 12 and 18 the minimal sequence requirements for trichogin GA IV activity were also reported.

The experimental data accumulated on synthetic analogs considerably expanded our knowledge of the minimal structural requirements for membrane activity of this lipopeptaibol. We found that the substitution of the C-terminal 1,2-amino alcohol (Lol) by the corresponding α-amino methyl ester (Leu-OMe) affects only marginally the biological properties of trichogin GA IV.[12] Conversely, the N$^\alpha$-blocking fatty acyl moiety was shown to play a major role in its membrane modifying properties.[12] More specifically, at least six carbon atoms in the aliphatic chain are required for a significant membrane activity. By use of a set of N$^\alpha$-octanoylated peptides of increasing main-chain length (from the C-terminus), it was established that membrane permeability properties, although weak, begin at a main-chain length as short as the tetrapeptide, and progressively increase up to the full length of the peptide.[18] A significant influence of the three Aib residues is also evident. It is clear that the extent of membrane activity and the amount of folding run roughly parallel, in the sense that largely folded, but not helical, conformers are typically present in the short sequences, while the longest peptides exhibit regular helical structures. We are currently actively investigating details of the self-aggregation process and the mechanism of action of trichogin GA IV in the membranes under a variety of experimental conditions, using not only sensitive fluorescence and EPR techniques[26–44] but solid-state NMR[45] and other biophysical methods[46,47] as well. Recently, using a large set of proteolytic enzymes, we also provided clear evidence that trichogin GA IV is remarkably stable towards biocatalyzed hydrolysis.[48]

Since it is widely recognized that short, membrane active, resistant to protease degradation, cationic and amphiphilic peptides are extremely promising agents in the framework of modern anti-infective therapeutic strategies,[1–3] we decided: (i) to take advantage of the trichogin GA IV sequence as a template for the preparation of novel antibacterial peptaibols with improved bioproperties and (ii) to enhance the weak hydrophilicity of one of its faces (characterized by four Gly) by incorporation of one, two, three or four side-chain positively charged Lys residues. In one of these analogs, we aimed at reinforcing helicity upon replacement of one central Gly with an Aib residue.

## Results and discussion

### Peptide synthesis and characterization

In this work, we firstly synthesized by solution methods two Lys-monosubstituted, C-terminal [Leu$^{11}$-OMe] trichogin GA IV analogs, herein referred to as **K2-OMe** and **K9-OMe** (Table 1), in which a Gly residue (at position 2 or 9, respectively) was replaced by Lys. The synthetic approach in solution phase was initially preferred because of the well known poor reactivity of the Aib residues (three of them occur in the trichogin GA IV sequence) when located at the N-terminus in the peptide coupling reactions.[49] To perform these syntheses, we employed the segment condensation approach, which allows a faster preparation of multiple analogs than the step-by-step procedure. An important feature, which makes trichogin GA IV a versatile synthetic platform, is the presence of as many as seven achiral (Aib or Gly) residues spread all over its primary structure, which allow one to design suitable segments with an achiral residue at their C-termini, thus reducing the risk of epimerization during coupling reactions. Schemes 1 and 2 describe our synthetic strategy. To synthesize the target peptide sequence **K2-OMe** (Scheme 1), we split it in three short segments. Segments **C** (1–4), containing Lys$^2$(Z) where Z is benzyloxycarbonyl, and **B** (5–8) were designed as to have an achiral Aib residue at their C-termini. Then, segment **B** was condensed on segment **A** (9–11) and segment **C** was reacted on the resulting segment **B–A** (5–11). To synthesize peptide **K9-OMe** (Scheme 2), we followed a similar strategy [*via* segments **E**(1–4), **B**(5–8), and **D**(9–11), the latter containing Lys$^9$(Z), and **E–B**(1–8)]. The **B** segment is common to both synthetic strategies. The two **K2-OMe** and **K9-OMe** analogs were obtained in an overall yield of 18 and 25%, respectively. For the details of the synthetic procedures and characterizations of these analogs (and their synthetic precursor segments as well), see the Experimental section. Table 1 and Fig. 1 give details of their RP-HPLC profiles.

**Table 1** Amino acid sequences and HPLC retention times of trichogin GA IV and its analogs investigated in this work[a]

| Abbreviation | Sequence | $t_R$/min[b] |
|---|---|---|
| **TRIC** | *n*-Oct-Aib$^1$-Gly$^2$-Leu$^3$-Aib$^4$-Gly$^5$-Gly$^6$-Leu$^7$-Aib$^8$-Gly$^9$-Ile$^{10}$-Lol | 17.7 |
| **K5** | *n*-Oct-Aib-Gly-Leu-Aib-**Lys**$^5$-Gly-Leu-Aib-Gly-Ile-Lol | 17.6 |
| **K6** | *n*-Oct-Aib-Gly-Leu-Aib-Gly-**Lys**$^6$-Leu-Aib-Gly-Ile-Lol | 16.1 |
| **K56** | *n*-Oct-Aib-Gly-Leu-Aib-**Lys**$^5$-**Lys**$^6$-Leu-Aib-Gly-Ile-Lol | 13.9 |
| **K259U6** | *n*-Oct-Aib-**Lys**$^2$-Leu-Aib-**Lys**$^5$-**Aib**$^6$-Leu-Aib-**Lys**$^9$-Ile-Lol | 15.2 |
| **K2569** | *n*-Oct-Aib-**Lys**$^2$-Leu-Aib-**Lys**$^5$-**Lys**$^6$-Leu-Aib-**Lys**$^9$-Ile-Lol | 9.5 |
| **K2-OMe** | *n*-Oct-Aib-**Lys**$^2$-Leu-Aib-Gly-Gly-Leu-Aib-Gly-Ile-**Leu-OMe** | 14.8 |
| **K9-OMe** | *n*-Oct-Aib-Gly-Leu-Aib-Gly-Gly-Leu-Aib-**Lys**$^9$-Ile-**Leu-OMe** | 18.3 |

[a] Single-letter amino acid abbreviations include: lysine (K) and α-aminoisobutyric acid (U). [b] $t_R$: retention time in RP-HPLC, using the conditions described in the Experimental section.

 

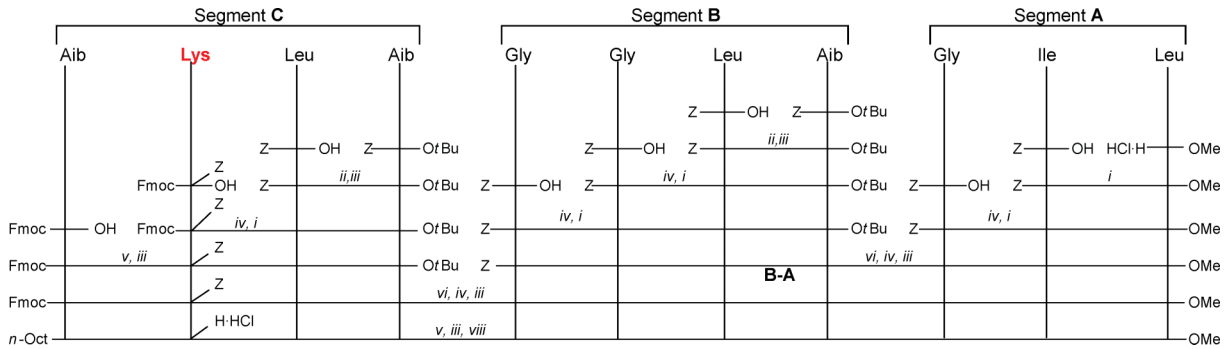


**Scheme 1** Synthetic strategy adopted for the synthesis of peptide **K2-OMe**: (i) HOBt, EDC in distilled $CH_2Cl_2$, pH kept at 8 by adding NMM; (ii) $H_2$, Pd/C (20%) in distilled $CH_2Cl_2$. (iii) HOAt, EDC in distilled $CH_2Cl_2$, pH kept at 8 by adding NMM; (iv) $H_2$, Pd/C (10%) in $CH_3OH$; (v) DEA (20 eq.) in distilled $CH_2Cl_2$; (vi) TFA (10 eq.) in distilled $CH_2Cl_2$; (vii) *n*-Oct-OH, HOAt, EDC, in distilled $CH_2Cl_2$, pH kept at 8 by adding NMM; (viii) $H_2$, Pd/C (10%) in $CH_3OH$, HCl 3 M in $CH_3OH$.

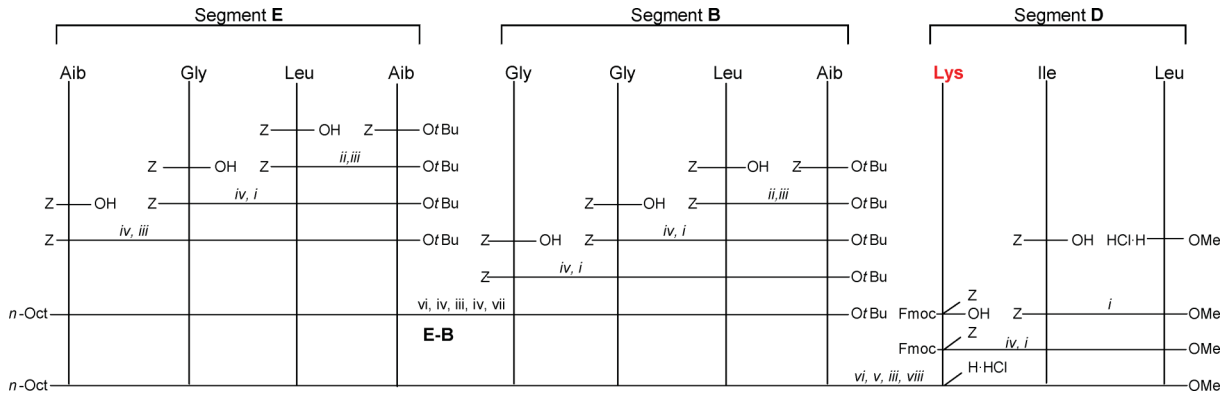


**Scheme 2** Synthetic strategy adopted for the synthesis of peptide **K9-OMe**. Solvents and reagents are those reported in Scheme 1. Segment B is common to both strategies.

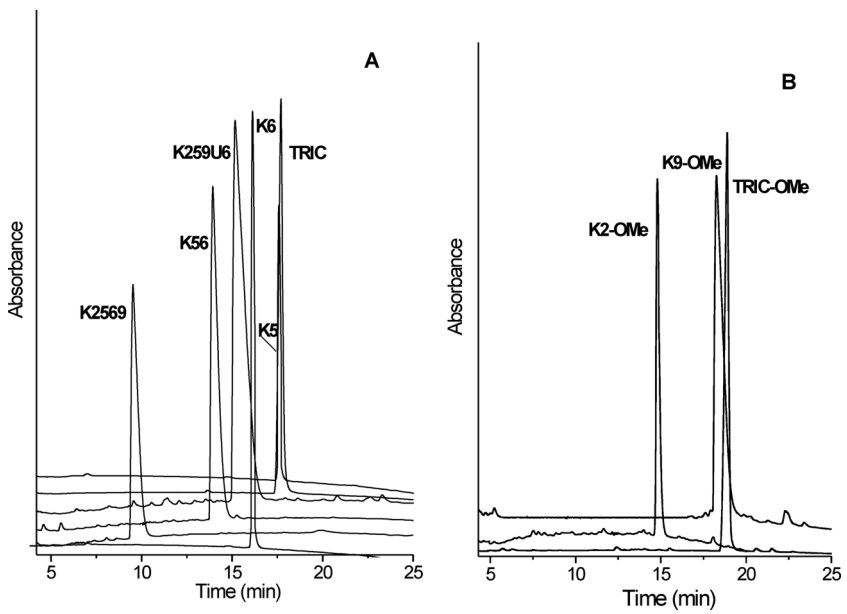


**Fig. 1** RP-HPLC profiles obtained for the purified SPPS-produced trichogin GA IV and its **K5**, **K6**, **K56**, **K259U6**, and **K2569** analogs (**A**) and for the **K2-OMe** and **K9-OMe** analogs produced by peptide synthesis in solution (**B**). [Leu[11]-OMe]-trichogin GA IV (Tric-OMe)[12] is reported as reference.

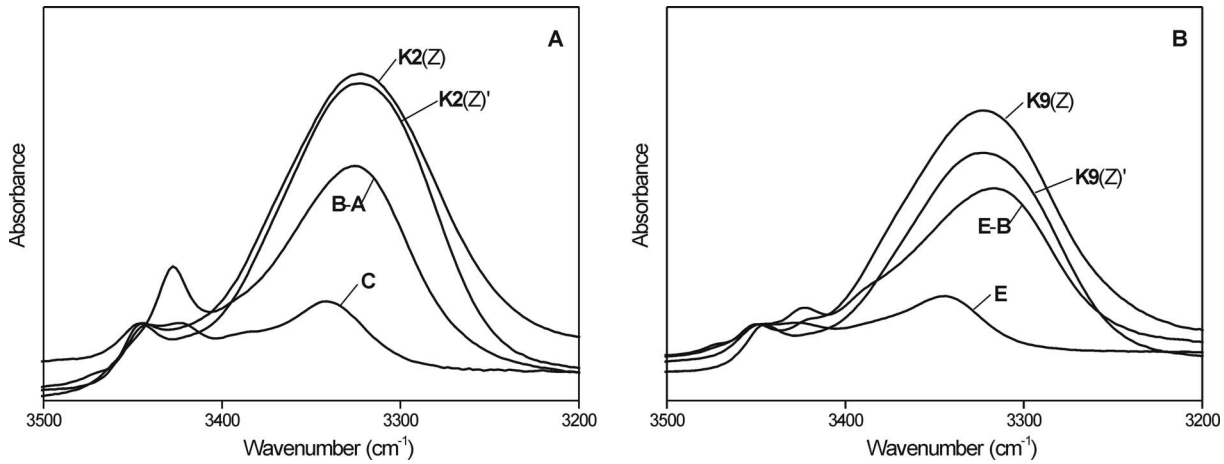


**Fig. 2** FT-IR absorption spectra (3500–3200 $cm^{-1}$ region) in $CDCl_3$ solution of the $N^{\varepsilon}$-Lys Z-protected **K2-OMe** and **K9-OMe** trichogin GA IV analogs at 1 mM [curves labeled **K2**(Z) in **A** and **K9**(Z) in **B**] and 0.1 mM [curves labeled **K2**(Z)′ in **A** and **K9**(Z)′ in **B**] peptide concentrations. The spectra of the shorter peptides (**C** and **B–A** in **A**, and **E** and **E–B** in **B**) at 0.1 mM peptide concentration are also shown.

Although the solution-phase procedure afforded the two desired analogs in good amounts, and allowed us to study the conformational properties of their synthetic segments as well, it was significantly time consuming. For this reason, we decided to make use of our improved protocol for automatic solid-phase peptide synthesis (SPPS), developed for the synthetically difficult medium-length peptaibiotic heptaibin,[50] to prepare trichogin GA IV and its five analogs **K5**, **K6**, **K56**, **K259U6** and **K2569** (Table 1) where the four Gly at position 2, 5, 6 and 9 were partially or fully replaced by Lys residues (in one of them $Gly^6$ was additionally substituted by Aib).

These syntheses, performed in parallel on the Lol-substituted 2-chlorotrityl resin[51,52] as described in the Experimental section, required 30 h only. After cleavage of the peptides from the resin, we collected the crude products, protected as *tert*-butyloxycarbonyl (Boc) derivatives at the side-chain of Lys residues, in about 90% purity. After purification by flash chromatography, the peptides were subjected to Boc removal using HCl in methanol. The desired final compounds were isolated in 42–50% yield with a purity >98%, as highlighted by RP-HPLC (Table 1 and Fig. 1). The peptides were additionally characterized by ESI-MS and NMR spectrometry (see Experimental section). The recently reported SPPS of trichogin GA IV, carried out according to a procedure partially different from that described here, resulted in a 20% isolated yield.[53]

### Conformational analysis

A detailed analysis of the conformational preferences of the seven Lys-containing trichogin GA IV analogs synthesized in this work was performed using FT-IR absorption, CD, and 2D-NMR spectroscopies in different solvents and environments.

As the **K2-OMe** and **K9-OMe** free Lys-containing peptides are only sparingly soluble in $CDCl_3$, we carried out the FT-IR absorption study on their synthetic precursors, namely the corresponding $N^{\varepsilon}$-Lys Z-protected compounds. This spectroscopic technique, although not providing definitive conformational conclusions, is able to offer useful initial hints. In the conformationally informative 3500–3200 $cm^{-1}$ region at 1.0 mM concentration, the two spectra are dominated by an intense absorption at 3330–3325 $cm^{-1}$, assigned to the N–H stretching mode of H-bonded peptide groups[54–56] (Fig. 2). An additional weak band is visible at about 3450 $cm^{-1}$, attributed to free (solvated) amide/peptide groups. A remarkable dilution effect is observed in the spectra of both peptides between 1.0 and 0.1 mM concentration (Fig. 2). We ascribe this difference to a strong tendency of the two analogs to self-aggregate above 0.1 mM concentration in this solvent. The spectra observed at the lowest concentration examined can be reasonably interpreted as arising almost exclusively from intramolecular C═O · · · H–N interactions. We conclude that these FT-IR absorption spectra are consistent with the hypothesis that in $CDCl_3$, a solvent of low polarity, at low concentration the preferred conformation of these two analogs, rich in the helix-supporting Aib residues,[20–23] would be highly folded and extensively stabilized by intramolecular H-bonds. These results parallel closely those already published for natural trichogin GA IV and its [$Leu^{11}$-OMe] analog.[12,15,16,18]

Fig. 2 also shows the spectra (peptide concentration: 1.0 mM) of the shorter segments **C**(1–4) and **B–A** (5–11) utilized for the synthesis of the $N^{\varepsilon}$-Lys Z-protected **K2-OMe** (part **A**), and **E**(1–4) and **E–B**(1–8) employed to prepare the $N^{\varepsilon}$-Lys Z-protected **K9-OMe** (part **B**). It is clear that in both series peptide main-chain elongation induces a substantial enhancement of the N–H stretching band of the H-bonded peptide groups relative to that of free peptide groups. Concomitantly, the frequency maximum of the former band shifts to lower wavenumbers. These findings represent an unambiguous evidence for the organization of the peptide chain into a secondary structure stabilized by intramolecular C═O · · · H–N H-bonds. Interestingly, among the four shorter segments, only **E–B** exhibits the concentration dependent effect (between 1.0 and 0.1 mM; Fig. S1†) which characterizes the IR absorption properties of the two mono-substituted trichogin GA IV Lys(Z) analogs. This result suggests that the tendency to self-associate is promoted by the presence of the N-terminal, long-chain, *n*-octanoyl amide group.

The far-UV CD spectra of the seven Lys-based trichogin GA IV analogs recorded in methanol (MeOH) and in water containing 100 mM sodium dodecylsulphate (SDS) at 0.1 mM peptide concentration are shown in Fig. 3. The corresponding

 

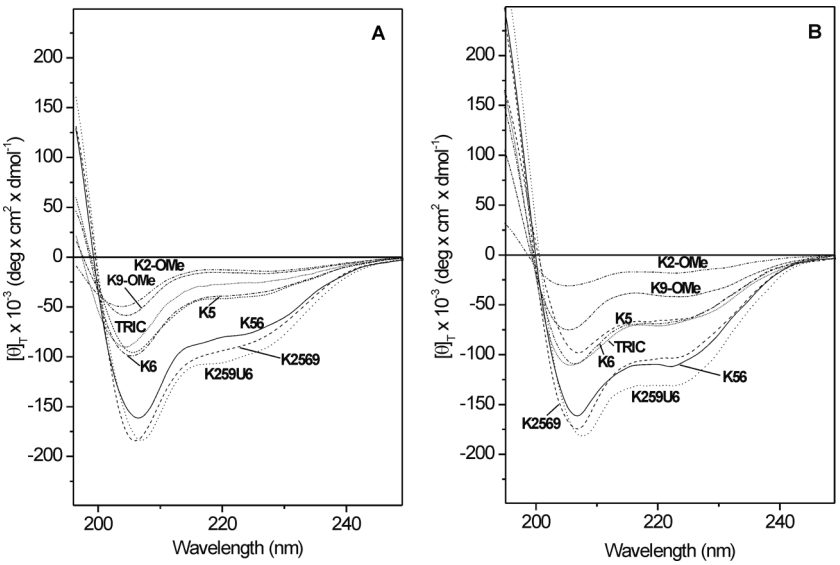


**Fig. 3** Far-UV CD spectra of trichogin GA IV and the seven Lys-based analogs in MeOH solution (**A**) and in aqueous solution containing 100 mM SDS (**B**). Peptide concentration: 0.1 mM.

spectra for the native peptaibol are reported for comparison (see also ref. 7,12,15,16,18). In both environments all peptides display a negative maximum at approximately 205 nm (parallel component of the exciton split $\pi \rightarrow \pi^*$ amide transition[57]) and a pronounced negative shoulder located at about 225 nm ($n \rightarrow \pi^*$ amide transition). These features are characteristic of peptides mainly structured in a right-handed helix. Although the shapes of all of the curves are similar, the ellipticity values vary significantly. This finding does not necessarily indicate a much higher helicity for the more substituted analogs (although this conclusion might also apply) because in these compounds one or more achiral Gly are replaced by chiral Lys residues. In this connection, it is worth noting that the ellipticity values exhibited by the **K2-OMe** and **K9-OMe** monosubstituted analogs are lower than those of trichogin GA IV. This latter result may suggest that the replacement of a Gly residue at either the N- or the C- terminus of the sequence is not beneficial for folding. However, it is worth remembering that the difference in the C-terminal moiety between the **K2-OMe** and **K9-OMe** analogs (Leu[11]-OMe carboxyl ester) and the other Lys-containing analogs (Lol 1,2-amino alcohol) might play a role as well.[7,12,15,16,18] Moreover, if the ratio (*R*) between the ellipticity values at 225 and 205 nm is considered,[58–60] it turns out clearly that for all peptides this parameter is enhanced (from 0.3–0.5 to 0.6–0.7) from MeOH to the membrane mimetic environment (SDS). On the basis of literature data, we interpret this result as arising from a contribution of mixed $3_{10}$-/$\alpha$-helical conformations with increasing $\alpha$-helix population in SDS micelles. However, increasing the temperature from 20 to 40 °C in aqueous SDS, the contribution of the α-helix to the conformational equilibrium mixture of the Lys tetrasubstituted analog **K2569** decreases (*R* value at 40 °C: 0.43, Fig. S2†). This result, while underscoring the thermal stability of the overall helical structure of this short peptide containing four cationic residues (37% of the overall sequence), also highlights its uncommon capability to undergo a transition between the $3_{10}$- and α- helical conformations.

We extended our CD analysis to aqueous solutions. In water at pH 5–6 (Fig. 4A) the spectra of the seven analogs (trichogin GA IV is not soluble in water), all similar in shape (*R* values between 0.4 and 0.5) and with only a limited variation in the ellipticity values, reflect the propensity of the peptides to adopt a helical conformation endowed with a predominant $3_{10}$-helical character. The only exception is represented by **K5** which seems to adopt a slightly more populated α-helical conformation ($R = 0.65$). Interestingly, in phosphate buffer the CD curves of the analogs containing two or more Lys residues change substantially from pH 3 to 11 (Fig. 4B). In particular, a dramatic variation is experienced by the **K2569** analog. Its CD profile at pH 3 (*R* value 0.3), where all four Lys side chains are protonated,[61,62] is clearly indicative of a well developed $3_{10}$-helical structure (for this analog the $3_{10}$-helix extent at pH 3 is even higher than that in MeOH). However, at pH 11 (*R* value 0.95), where all four Lys side chains are essentially uncharged, the peptide is folded in a fully developed $\alpha$-helical structure. Fig. 5 highlights the intriguing phenomenon of a pH controlled, reversible $3_{10}$-helix to $\alpha$-helix conversion (from acidic to highly basic pH values and *vice versa*). At this point, it should be emphasized that this finding, never authenticated before in the literature for any peptaibol or analog thereof, implies a significant overall contraction (about 4 Å) of the peptide backbone following the conformational transition from the longer $3_{10}$-helix[24] to the shorter $\alpha$-helix and an associated generation of a biomolecular spring.

To study the lipopeptaibol conformation in more detail, an NMR analysis was performed. The 2D-NMR spectra of the three Lys-containing trichogin GA IV analogs, **K56**, **K2569**, **K259U6** were first acquired in $CD_3OH$. The complete assignments of the proton resonances were obtained following the Wüthrich procedure.[63] The ROESY spectra exhibit all of the sequential $NH_i \rightarrow NH_{i+1}$ cross peaks characteristic of the presence of an helical structure. In particular, the fingerprint region of the ROESY spectrum of **K2569** in $CD_3OH$ (Fig. 6A) shows four $C^{\alpha}H_i \rightarrow NH_{i+3}$ cross peaks, typical of the presence of a helical conformation, along with three $C^{\alpha}H_i \rightarrow NH_{i+4}$ and four $C^{\alpha}H_i \rightarrow NH_{i+2}$ cross peaks, which denote the presence of an α- and a $3_{10}$- helical conformation, respectively. The NMR analysis was extended to an aqueous solution (pH 3) (Fig. 6B) and a 100 mM SDS

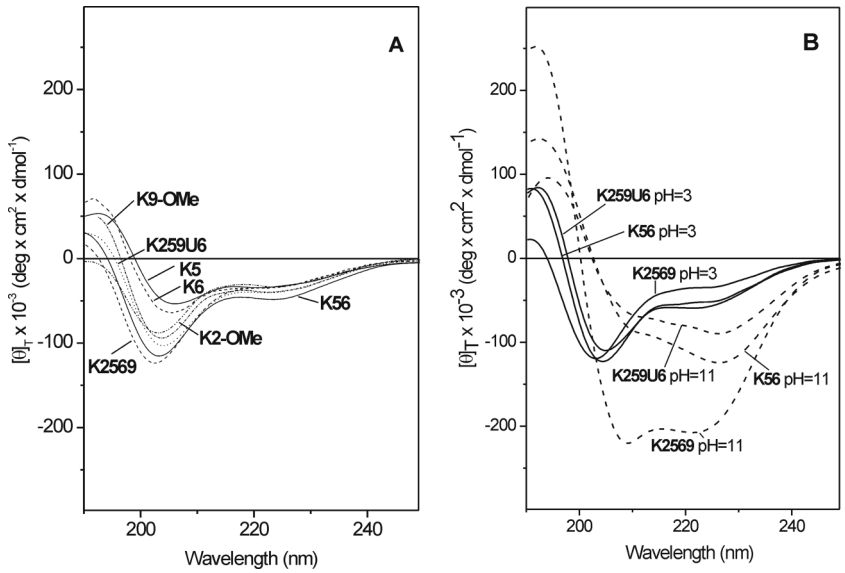


**Fig. 4** Far-UV CD spectra of the seven trichogin GA IV analogs in aqueous solution. (**A**) Spectra in water (pH 5–6). (**B**) Spectra of the **K56**, **K259U6**, and **K2569** analogs in phosphate buffer at pH 3 and 11. Peptide concentration: 0.1 mM.

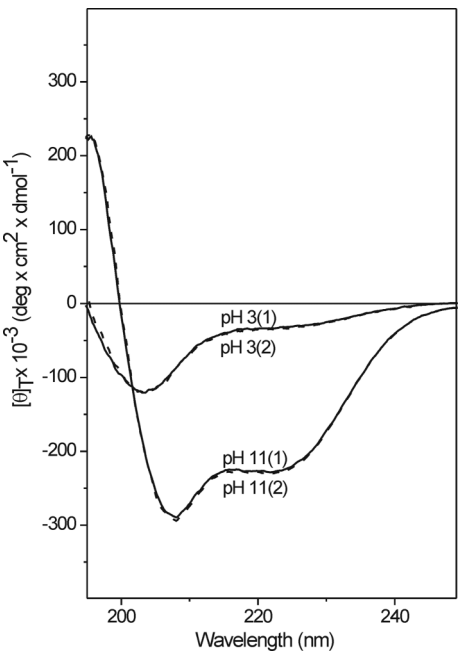


**Fig. 5** Far-UV CD spectra of the **K2569** trichogin GA IV analog in aqueous solution at pH 3 and 11. Repeated cycles of helix conversion were performed, the order of pH switches being pH 3 (1), pH 11 (1), pH 3 (2), and pH 11 (2). Peptide concentration: 0.015 mM.

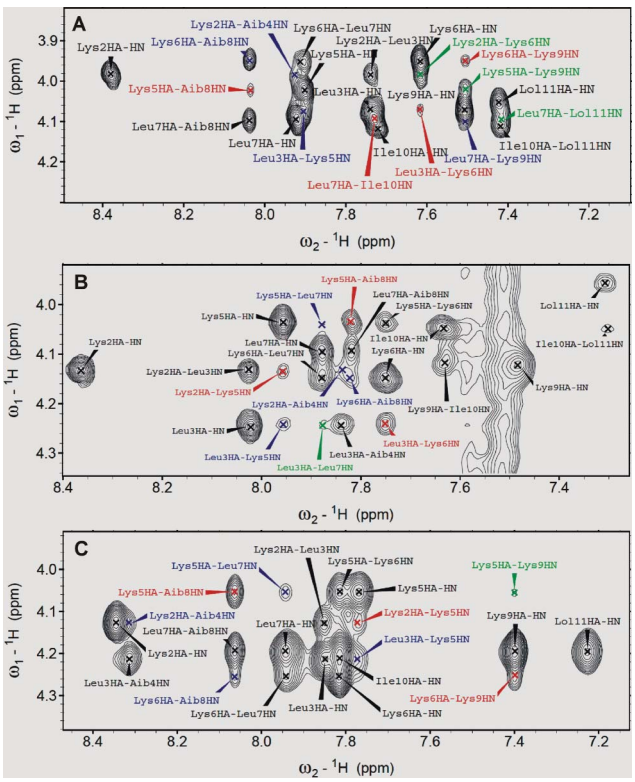


**Fig. 6** Fingerprint region of the ROESY/NOESY spectra of the **K2569** trichogin GA IV analog under three different conditions: (**A**) 5.6 mM in $CD_3OH$ (298 K, 600 MHz); (**B**): 1.8 mM in 9 : 1 $H_2O/D_2O$, pH 3 (303 K, 600 MHz); (**C**) 3.5 mM in 9 : 1 $H_2O/D_2O$ containing 100 mM SDS-$d_{25}$, pH 2.83 (313 K, 600 MHz). Medium-range interactions, diagnostic of the presence of a mixed $3_{10}$-/α-helical structure: in blu $C^{\alpha}H_i \rightarrow NH_{i+2}$ ($3_{10}$-helix); in green: $C^{\alpha}H_i \rightarrow NH_{i+4}$ (α-helix); in red: $C^{\alpha}H_i \rightarrow NH_{i+3}$ ($3_{10}$-/α-helix).

membrane-mimetic environment (pH 2.83) (Fig. 6C). Here, the $3_{10}$-helix contribution to the overall conformation is larger with respect to that of the $\alpha$-helix (four $C^{\alpha}H_i \rightarrow NH_{i+2}$ cross peaks *versus* only one $C^{\alpha}H_i \rightarrow NH_{i+4}$). The present findings highlight the occurrence of a mixed $3_{10}$-/$\alpha$-helical conformation in the three solvents examined, which is more markedly $3_{10}$-helical in the aqueous acidic environment. These results nicely confirm the CD observation discussed above. In particular, the CD spectra recorded at different temperatures explain the NMR observation of a prevailing $3_{10}$-helical structure in the membrane-mimicking environment at 40 °C (Fig. 6C). The NMR spectrum of this analog was not recorded at pH 11, where it is known to be fully

 

$\alpha$-helical (see above), because of the rapid exchange rate of the amide protons under basic conditions.

### Biological activity

The hemolytic activity of the seven Lys-containing trichogin GA IV analogs, a chronic handicap for most AMPs (including peptaibols),[64] was tested. The lytic concentrations causing 50% hemolysis ($LC_{50}$) after one hour incubation with 4% human red blood cells (hRBCs) in PBS, are reported in Table 2. From the biophysical properties summarized in Table 2, it is clear that the capability of trichogin GA IV analogs to kill hRBCs is correlated to the peptide hydrophobicity rather than to the total number of charges. Notably, the presence of an Aib residue at position 6 of **K259U6** analog seems to balance out the net charge, enhancing the compound hydrophobicity to a value greater than that of the **K56** analog. Not surprisingly, the hemolytic activity of these two analogs follows the same trend. This observation brings us to conclude that it might be possible to modulate the effect of cationic residues by strengthening the overall helical peptide conformation. From the RP-HPLC retention times of the monosubstituted analogs (Table 1), **K9-OMe** results to be even more hydrophobic than trichogin GA IV, probably because of the presence of the C-terminal methyl ester functionality. Moreover, even though **K5** and **K6** have the same net charge, they possess different hydrophobicities. Also in this case, the hemolytic activities follow the same trend, with **K5** being less toxic than **K6**. A particular effect of the C-terminal methyl ester is probably at the basis of the behavior of **K2-OMe** that, although less hydrophobic than the other monosubstituted analogs, exhibits a remarkably low hemolytic activity.

**Table 2** Biophysical properties of trichogin GA IV and its analogs

| Abbreviation | $MW_{calc}$ | $MW_{obs}$ | Q[a] | H (%)[b] | $LC_{50}$ (μg ml$^{-1}$)[c] |
|---|---|---|---|---|---|
| **TRIC** | 1065.72 | 1065.74 | 0 | 100 | >32 |
| **K5** | 1136.79 | 1136.77 | 1 | 99.4 | 16 |
| **K6** | 1136.79 | 1136.86 | 1 | 91.0 | 8 |
| **K56** | 1207.86 | 1207.86 | 2 | 78.5 | 5.4 |
| **K259U6** | 1306.97 | 1306.95 | 3 | 85.9 | 10 |
| **K2569** | 1350.01 | 1350.00 | 4 | 53.7 | 5.4 |
| **Tric-OMe**[12] | 1093.71 | 1093.72 | 0 | 100 | >32 |
| **K9-OMe** | 1164.78 | 1164.82 | 1 | 96.8 | >32 |
| **K2-OMe** | 1164.78 | 1164.81 | 1 | 78.3 | >32 |
| Melittin[d] | 2846.46 | 2846.46 | 5 | n.d.[e] | 2 |

[a] Q: total charge. [b] H: molecular hydrophobicity estimated from elution time in reversed-phase HPLC with respect to the native compound (**TRIC** or **Tric-OMe**). [c] $LC_{50}$: peptide concentration responsible for 50% hemolysis after 3 h incubation with 4% red blood cells in PBS. [d] Antimicrobial, hemolytic peptide used as standard (ref. 87). [e] n.d.: not determined.

The antimicrobial activity of the seven Lys-containing trichogin GA IV analogs was investigated against two strains of Gram-positive bacteria (*Staphylococcus aureus* and *Staphylococcus epidermidis*), two strains of Gram-negative bacteria (*Escherichia coli* and *Pseudomonas aeruginosa*), and two types of fungi (*Candida albicans* and *Trichosporon beigelli*). The minimum inhibitory concentration (MIC) values are reported in Table 3, together with the values found for the well-known antimicrobial peptide melittin under the same experimental conditions. In general, the presence of the positively charged Lys residues increases the antibacterial activity and broadens the spectrum of action of the analogs with respect to those of the native peptide. Among all analogs, **K56** shows a remarkable increased activity against all strains tested, while **K259U6** exhibits a specific, very strong activity against *S. aureus*. Remarkably, the presence of one or more Lys residues induces antifungal properties to all of the analogs of trichogin GA IV, which is a fungal peptide. The monosubstituted analogs allowed us to study the influence of the position of the Lys residue in the sequence on the biological properties. From Table 3 it is clear that the Lys position plays an important role. Indeed, while the antimicrobial action of **K2-OMe** closely parallels that of the native peptide and **K5** and **K6** show the same selectivity as that of trichogin GA IV, though somewhat enhanced, the **K9-OMe** analog exhibits a broader antibacterial spectrum, with a remarkable activity against both the Gram-positive strains tested and the Gram-negative *E. coli*. This analog also shows a very promising selectivity for bacteria with respect to hRBCs. We also tested the cytotoxicity of **K9-OMe** against HaCaT (Human adult low-Calcium high Temperature keratinocyte cells) and found little toxicity (> 64 μg ml$^{-1}$).

Analyzing in depth the MIC values reported in Table 3, we can make an attempt to establish a relationship between the number of Lys residues and the overall antimicrobial activity of the trichogin GA IV analogs. The substitution of either $Gly^5$ or $Gly^6$

**Table 3** Antimicrobial activities (MIC values) of trichogin GA IV and its analogs[a]

| | Bacteria | | | | | |
|---|---|---|---|---|---|---|
| | Gram-positive | | Gram-negative | | Fungi | |
| Peptide | *S. aureus* | *S. epidermidis* | *E. coli* | *P. aeruginosa* | *C. albicans* | *T. beigelli* |
| **TRIC** | 8–16 | >64 | 32 | >64 | >64 | >64 |
| **K5** | 4 | 64 | 4 | 64 | 8 | 8 |
| **K6** | 4 | 64 | 4 | 64 | 16 | 8 |
| **K56** | 4 | 4 | 4 | 4 | 4 | 4 |
| **K259U6** | 2 | 8 | 8 | 8 | 16 | 4 |
| **K2569** | 8 | 8 | 8 | 8 | 8 | 8 |
| **K2-OMe** | 4 | 64 | 32 | 32 | 64 | 32 |
| **K9-OMe** | 4 | 4 | 8 | 64 | 64 | 64 |
| **Tric-OMe**[12,48] | 16 | >64 | 32 | >64 | n.d.[c] | n.d.[c] |
| Melittin[b] | 4 | 2 | 2 | 4 | 8 | 8 |

[a] All values are in μg ml$^{-1}$. [b] Antimicrobial peptide used as standard. [c] n.d.: not determined.

with Lys dramatically increases the toxicity of this peptaibiotic against *S. aureus* and *E. coli*. The concomitant substitution of both those Gly residues does not improve the activity against the two above mentioned strains, thus excluding the presence of a cooperative effect between the two positive charged residues in the peptide mechanism of action against these two bacteria. The picture changes if we look at the MIC values obtained against the other bacteria tested. Indeed, it seems that, in order to broaden the spectrum of the antimicrobial action of trichogin GA IV, at least two Gly residues must be replaced by Lys. This conclusion is further confirmed by the selectivity shown by the other monosubstituted analogs **K2-OMe** and **K9-OMe**. Moreover, the presence of additional positively charged residues does not further reduce the MIC values, which, for the **K259U6** and **K2569** analogs, are almost comparable to those of **K56**.

In summary: (i) the insertion of an Aib residue may modulate the biological properties of cationic peptides; (ii) it is not only the net charge that is responsible for the enhanced antimicrobial properties of trichogin GA IV analogs, but the position of the Lys residue(s) in the primary structure as well; (iii) the **K9-OMe** analog is a very promising antimicrobial agent, as it possesses a 7-fold greater activity against bacteria than against hRBCs.

### Membrane activity

The membrane permeability properties of most of the synthetic analogs were at first tested in comparison with the native lipopeptaibol trichogin GA IV by measuring the induced leakage of 5(6)-carboxyfluorescein (CF) entrapped in small unilamellar vesicles (SUVs). For this investigation, the overall neutral, zwitter-ionic 1,2-dioleyl-*sn-glycero*-3-phosphocholine (DOPC)/cholesterol (Ch) model membrane was exploited. The permeability effect of the Lys-containing trichogin GA IV analogs is quite remarkable and close to that of the native compound (Fig. S3, Supporting Information†).[7,12]

To further investigate the mechanism of antimicrobial action of these novel peptaibiotics, we performed depolarization leakage assays on *S. aureus* and *E. coli* membranes. As shown in Fig. 7, the trend of their ability to induce membrane depolarization parallels their antimicrobial activities. In particular, the selective action of **K2-OMe** against *S. aureus* as compared to that against *E. coli* is reflected by its higher ability to induce depolarization of the related, former membrane. These results underscore the important role played by peptide · · · membrane interactions on the antimicrobial mechanism of the trichogin GA IV analogs. Indeed, the ability of these compounds to interact with the membrane bilayer is likely to be mainly responsible for their biological activity and makes them promising candidates as new antimicrobial agents with reduced resistance-induction risks.

### Proteolytic stability

We assessed the resistance of trichogin GA IV analogs to the action of several proteolytic enzymes.[65–72] The Lol-containing analogs proved to be resistant towards the proteolysis of pronase E, subtilisin and papain for more than four hours. However, the C-terminal methyl esters of the monosubstituted **K2-OMe** and **K9-OMe** analogs were hydrolyzed to the corresponding free carboxylic acids within 15 min, as proved by isolation and characterization of the products by ESI-MS. The resulting free carboxylic acid peptides were stable towards further proteolysis for more than four hours. All of the analogs were extensively digested by trypsin within 15 min, except **K2-OMe** and **K6** which are surprisingly resistant to the action of this enzyme, with an half-life time of two and three hours, respectively (Fig. 8).

## Conclusions

The most extensively studied short peptaibiotic is trichogin GA IV, a 10-amino acid peptide characterized by the presence of a fatty acid chain (*n*-octanoyl) at its N-terminus and a C-terminal 1,2-amino alcohol. Its mechanism of action on the membranes is under debate, even if it is clearly driven by its stable, mixed $3_{10}$-/α- helical conformation. In this paper, we enhanced the natural modest amphiphilic character of the trichogin GA IV 3D-structure by replacing one or more Gly, lying on the same face of the helix, by Lys residues. To determine the conformational preferences in solution of the peptaibiotics synthesized, we subjected them to a thorough investigation by means of IR absorption, CD, and 2D NMR in various solvents and in a membrane-mimetic

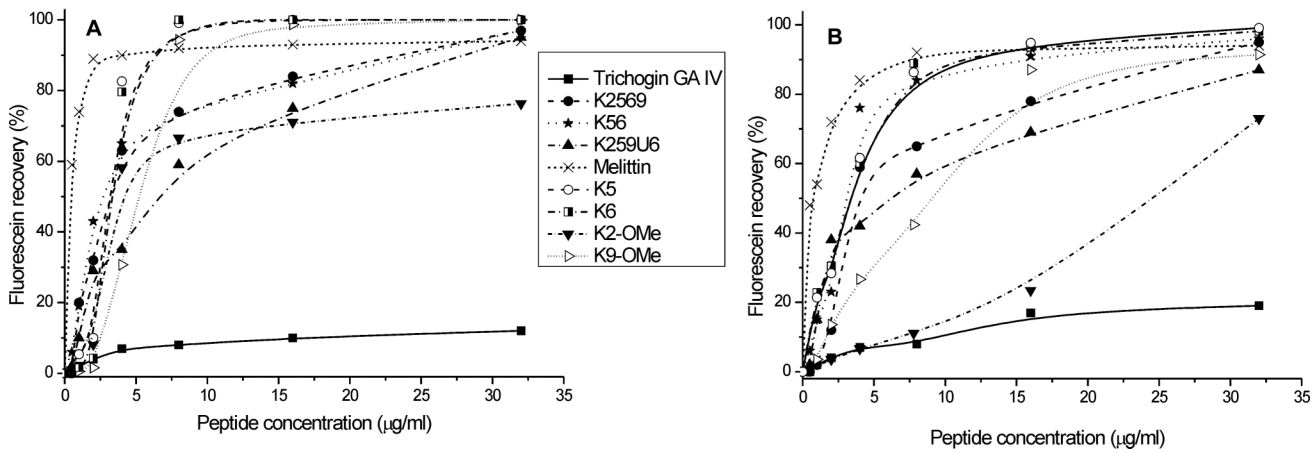


**Fig. 7** Peptide-induced depolarization of bacterial membranes. Each peptide was added to *S. aureus* (**A**) or *E. coli* (**B**) bacteria previously pre-equilibrated for 60 min with $DiSC_3$-5. Fluorescence recovery was measured in continuous after peptide incorporation. The maximum fluorescence recovery values are shown for each peptide.

 

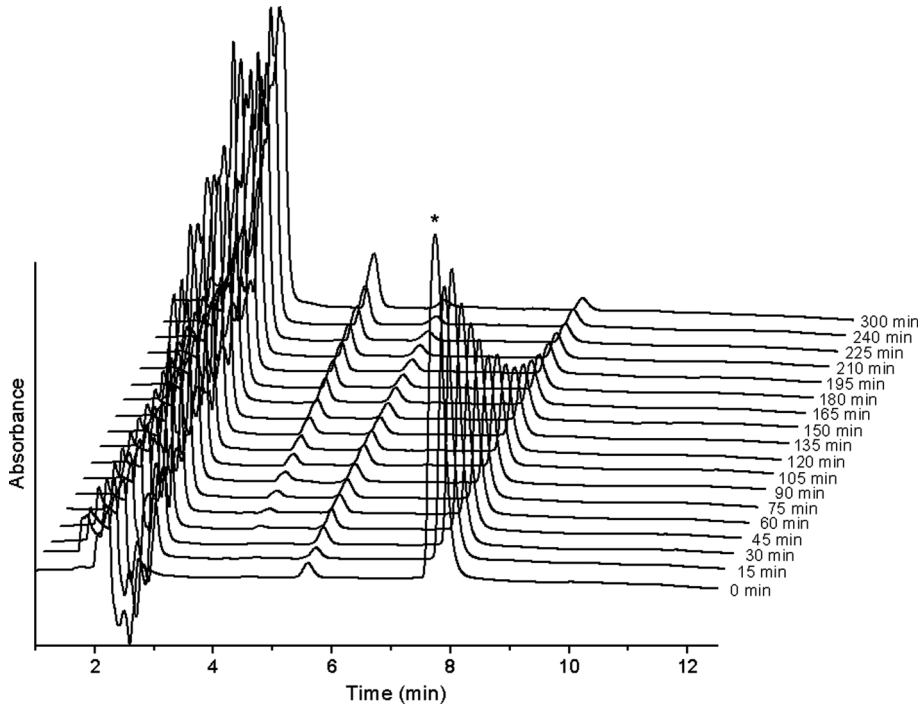


**Fig. 8** RP-HPLC profiles obtained for the **K2-OMe** trichogin GA IV analog in presence of the proteolytic enzyme trypsin, checked every 15 min. Elution conditions: column: Phenomenex Kromasil 100 Å, 5 μm; flux: 1 ml $min^{-1}$; gradient: 70–90% B in 10 min; eluant A: 9 : 1 $H_2O/CH_3CN$ + 0.05% TFA; eluant B: 9 : 1 $CH_3CN/H_2O$ + 0.05% TFA. The initial peak for **K2-OMe** is starred.

environment. The Lys-containing analogs exhibit a stable helical conformation, which can be intriguingly switched from $3_{10}$- to α-helix by changing the pH from 3 to 11. The critical pH for the transition, which is located between 9 and 10 (far above the physiological pH conditions), seems to exclude a possible role for this conformational switch on the mechanism of the antimicrobial action of our analogs. The fluorescence and depolarization leakage experiments reveal that the novel peptaibiotics retain the native capability to interact with model membranes. The sensitivity assays *in vitro* against a collection of bacteria (both Gram-positive and Gram-negative) and fungal species of clinical relevance assessed on the synthetic analogs underscored their broad antimicrobial spectrum. However, the presence of more that one Lys residue increases the hemolytic activity and shorten the resistance toward trypsin digestion. To summarize, the Lys-containing, short peptides described herein (particularly the most substituted ones) could find applications as molecular switches,[73] for their uncommon ability to undergo pH-mediated, reversible, conformational transitions. More importantly, in our view, two of the least substituted analogs, **K9-OMe** for its broad antimicrobial spectrum and low cytotoxicity and **K2-OMe** for its uncommon tryptic resistance, may represent promising leads for the development of new membrane-disrupting antimicrobial agents.

## Experimental

### Peptide synthesis and characterization

**General methods.** Melting points were measured by means of a capillary tube immersed in an oil bath (Tottoli apparatus, Büchi) and are uncorrected. Optical rotations $[\alpha]_D^{20}$ (given in units of $10^{-1}$ deg $cm^2$ $g^{-1}$) were measured at 20 °C on a Perkin-Elmer PE241 polarimeter using a 1 dm path length cell, at the D-wavelength of sodium (589 nm). The concentration of each compound (*c*) is given in mg $cl^{-1}$. Mass spectra (electrospray ionization, ESI-MS) was performed by using a PerSeptive Biosystem Mariner instrument (Framingham, MA). Analytical TLC and preparative column chromatography were performed on Kieselgel F 254 and Kieselgel 60 (0.040–0.063 mm) (Merck), respectively. The retention factor (Rf) values were determined using four solvent mixtures as eluants: $Rf_1$: chloroform/ethanol 9 : 1; $Rf_2$: 1-butanol/acetic acid/water 3 : 1 : 1; $Rf_3$: toluene/ethanol 7 : 1; $Rf_4$: methylene chloride/ethanol 9 : 1.

Fmoc(9-fluorenylmethyloxycarbonyl)-amino acids were supplied by Novabiochem (Merck Biosciences, La Jolla, CA). All other amino acid derivatives and reagents for peptide synthesis were purchased from Sigma-Aldrich (St. Louis, MO). The final products were characterized by analytical RP-HPLC on a Vydac $C_{18}$ column (4.6 × 250 mm, 5 μ, 300 Å) using a Dionex (Sunnyvale, CA) P680 HPLC pump with an ASI-100 automated sample injector. The binary elution system used was: A, 0.1% TFA in $H_2O$; B, 0.1% TFA (trifuoroacetic acid) in $CH_3CN/H_2O$ (9 : 1 v/v); gradient 50%–90% B in 20 min (flow rate 1.5 ml $min^{-1}$); spectrophotometric detection at $\lambda = 216$ nm.

**Solution-phase peptide synthesis.** The peptide segments were obtained step-by-step using orthogonal, terminal- and side-chain protecting groups (Scheme 1). Removals of the Z and Fmoc $N^{\alpha}$-protections were achieved using Pd-catalyzed hydrogenation and diethylamine in methylene chloride followed by flash chromatography, respectively. In either the Xxx-Aib or the Aib-Xxx peptide

bond formation, C-activation was carried out using EDC, *N*-[3-(dimethylamino)-propyl]-*N′*-ethylcarbodiimide/HOAt (7-aza-1-hydroxy-1,2,3-benzotriazole)[74] procedure, while the EDC/HOBt (1-hydroxy-1,2,3-benzotriazole)[75] procedure, although less efficient for difficult couplings, was appropriate for the formation of the other peptide bonds. Every coupling reaction was performed with a 10% excess of the incoming residue. The pH of the coupling mixtures were kept at 8 by adding *N*-methylmorpholine. The C-terminal *tert*-butyl (O*t*Bu) esters were converted to free carboxylic acids upon treatment with diluted TFA in methylene chloride. The segment condensation reactions were obtained by EDC/HOAt C-activation, using a 10% excess of the C-terminal carboxyl free segment. The yields of the segment condensation reactions were about 50%. After each coupling reaction, the product was purified by flash chromatography using suitable ratios of methylene chloride/methanol or ethyl acetate/hexane mixtures.

**Segment A (Z-Gly-Ile-Leu-OMe):[12].** Overall yield: 76%. Melting point: 119-120 °C. $Rf_1$: 0.85, $Rf_2$: 0.95, $Rf_3$: 0.30. $[\alpha]_D^{20}$: –45.9° (*c* = 0.5, MeOH). IR (KBr): 3290, 1745, 1703, 1676, 1637, 1537 $cm^{-1}$. ESI-MS *m/z*: calculated for $C_{23}H_{35}N_3O_6$ 449.25, found 449.25. $^1H$ NMR (200 MHz, $CDCl_3$): $\delta$ 7.35 [m, 5H, Z phenyl CH], 6.64 [d, 1H, Ile NH], 6.35 [d, 1H, Leu NH], 5.48 [t, 1H, Gly NH], 5.13 [s, 2H, Z $CH_2$], 4.58 [m, 1H, Leu α-CH], 4.34 [m, 1H, Ile α-CH], 3.90 [m, 2H, Gly α-$CH_2$], 3.72 [s, 3H, OMe $CH_3$], 1.85 [m, 1H, Ile β-CH], 1.70–1.40 [m, 4H, Leu β-$CH_2$, Leu γ-CH, Ile 1 γ-CH], 1.13 [m, 1H, Ile 1 γ-CH], 1.00–0.80 [m, 12H, Leu 2 δ-$CH_3$, Ile γ-$CH_3$, Ile δ-$CH_3$]. $^{13}C$ NMR (150 MHz, $CDCl_3$): $\delta$ 173.042, 171.051, 169.055 [3s, ester and amide *C*═O], 156.557 [s, urethane *C*═O], 136.223 [s, aromatic quaternary *C*], 128.449, 128.420, 128.097, 128.001 [4s, aromatic *C*], 66.999 [s, urethane *C*$H_2$], 57.507, 52.144, 50.803, 44.339 [4s, $^{\alpha}C$ and -O*C*$H_3$], 40.996 [s, Leu $^{\beta}C$], 37.518 [s, Ile $^{\beta}C$], 24.840, 23.236, 22.618, 21.872 [4s, Ile $^{\gamma}C$, Leu $^{\gamma}C$ and $^{\delta}C$], 15.072, 11.176 [2s, Ile $^{\gamma}C$ and $^{\delta}C$].

**Segment B (Z-Gly-Gly-Leu-Aib-O*t*Bu).** Overall yield: 52%. Melting point: 67–68 °C. $Rf_2$: 0.95, $Rf_3$: 0.40, $Rf_4$: 0.75. $[\alpha]_D^{20}$: –22.1° (*c* = 0.5, MeOH). IR (KBr): 3312, 1732, 1711, 1651, 1535 $cm^{-1}$. ESI-MS *m/z*: calculated for $C_{26}H_{40}N_4O_7$ 520.29, found 520.29. $^1H$ NMR (400 MHz, $CDCl_3$): $\delta$ 7.35 [m, 5H, Z phenyl CH], 6.94 [t, 1H, $Gly^2$ NH], 6.81 [s, 1H, Aib NH], 6.67 [d, 1H, Leu NH], 5.61 [t, 1H, $Gly^1$ NH], 5.13 [s, 2H, Z $CH_2$], 4.40 [m, 1H, Leu α-CH], 4.00–3.80 [m, 4H, Gly α-$CH_2$], 1.63 [m, 3H, Leu β-$CH_2$, Leu γ-CH], 1.50 [s, 6H, Aib β-$CH_3$], 1.43 [s, 9H, O*t*Bu], 0.92 [m, 6H, Leu δ-$CH_3$]. $^{13}C$ NMR (100 MHz, $CDCl_3$): $\delta$ 173.469, 170.981, 169.598, 168.642 [4s, amide and ester *C*═O], 156.737 [s, urethane *C*═O], 136.063 [s, aromatic quaternary *C*], 128.531, 128.237, 128.073 [3s, aromatic *C*], 81.524 [s, O*t*Bu quaternary *C*], 67.228 [s, urethane *C*$H_2$], 56.904, 51.929, 44.455, 43.000 [4s, $^{\alpha}C$], 41.496 [s, $^{\beta}C$], 27.791 [s, O*t*Bu *C*$H_3$], 24.706, 24.534, 24.425 [3s, Leu $^{\gamma}C$, Aib $^{\beta}C$], 22.894, 22.006 [2s, Leu $^{\delta}C$].

**Segment C [Fmoc-Aib-Lys(Z)-Leu-Aib-O*t*Bu].** Overall yield: 50%. Oil. $Rf_2$: 0.95, $Rf_3$: 0.50, $Rf_4$: 0.85. $[\alpha]_D^{20}$: –21.5° (*c* = 0.5, MeOH). IR (KBr): 3317, 1700, 1658, 1525 $cm^{-1}$. ESI-MS *m/z*: calculated for $C_{47}H_{63}N_5O_9$ 841.46, found 841.46. $^1H$ NMR (400 MHz, $CDCl_3$): $\delta$ 7.77 [d, 2H, Fmoc], 7.56 [t, 2H, Fmoc], 7.40 [t, 2H, Fmoc], 7.31 [m, 5H, Z phenyl CH], 7.26 [m, 1H, NH], 6.87 [s, 1H, NH], 6.67 [m, 1H, NH], 5.00 [m, 3H, 1 Lys ε-NH and urethane $CH_2$], 4.58 [m, 1H, α-CH], 4.37 [m, 1H, α-CH], 4.13 [m, 2H, urethane $CH_2$], 3.16 [d, 2H], 1.85 [s, 6H], 1.64 [m, 3H, Leu β-$CH_2$, Leu γ-CH], 1.45 [m, 12H, Aib β-$CH_3$], 1.43 [s, 9H, O*t*Bu], 0.82 [m, 6H, Leu δ-$CH_3$]. $^{13}C$ NMR (100 MHz, $CDCl_3$): $\delta$ 175.349, 173.548, 171.460, 171.383 [4s, ester and amide *C*═O], 157.139, 156.015 [2s, urethane *C*═O], 143.513, 143.383, 141.387, 136.607 [4s, aromatic quaternary *C*], 128.598, 128.101, 127.917, 127.626, 127.160, 127.092, 124.920, 124.700, 120.123 [9s, aromatic *C*], 80.537 [s, O*t*Bu quaternary *C*], 66.875, 66.403 [2s, urethane *C*$H_2$], 56.984, 56.416, 54.983, 51.926 [4s, $^{\alpha}C$], 47.056 [s, Fmoc tertiary *C*], 39.943, 39.781 [2s, Leu $^{\beta}C$ and Lys $^{\varepsilon}C$], 30.247, 29.709, 29.624 [3s, Lys $^{\beta}C$, Lys $^{\delta}C$], 27.843 [s, O*t*Bu *C*$H_3$], 26.548, 25.081, 24.938, 24.532, 24.091 [5s, Leu $^{\gamma}C$, 4 Aib $^{\beta}C$], 23.263, 22.741, 21.012 [3s, Lys $^{\gamma}C$ and Leu $^{\delta}C$].

**Segment D [Fmoc-Lys(Z)-Ile-Leu-OMe].** Overall yield: 69%. Melting point: 192–194 °C. $Rf_2$: 0.95, $Rf_3$: 0.65, $Rf_4$: 0.95. $[\alpha]_D^{20}$:–43.8° (*c* = 0.5, MeOH). IR (KBr): 3294, 1693, 1642, 1536 $cm^{-1}$. ESI-MS *m/z*: calculated for $C_{42}H_{54}N_4O_8$ 742.40, found 742.37. $^1H$ NMR (600 MHz, $CDCl_3$): $\delta$ 7.75 [d, 2H, Fmoc], 7.58 [t, 2H, Fmoc], 7.49 [m, 2H, Fmoc], 7.32 [m, 5H, Z phenyl CH], 6.64 [d, 1H, NH], 6.36 [d, 1H, NH], 5.96 [d, 1H, NH], 5.07 [m, 2H, urethane $CH_2$], 4.60 [s, 1H, Lys ε-NH], 4.39 [m, 2H, urethane $CH_2$], 4.29 [t, 1H, α-CH], 4.20 [m, 2H, α-CH], 3.70 [s, 3H, -OMe $CH_3$], 3.20 [d, 2H], 1.80–1.38 [m, 5H, Leu β-$CH_2$, Leu γ-CH and Ile γ-$CH_2$], 0.89 [m, 12H, Leu δ-$CH_3$, Ile γ-$CH_3$ and δ-$CH_3$]. $^{13}C$ NMR (100 MHz, $CDCl_3$): $\delta$ 173.069, 171.813, 170.790 [3s, ester and amide *C*═O], 159.557, 156.735 [2s, urethane *C*═O], 143.776, 141.294, 136.608 [3s, aromatic quaternary *C*] 128.505, 127.750, 127.101, 125.037, 119.995 [5s, aromatic *C*], 67.156, 66.637 [2s, urethane *C*$H_2$], 57.950, 54.874, 53.540 [3s, $^{\alpha}C$], 52.279 [s, -O*C*$H_3$], 47.129 [s, Fmoc tertiary *C*], 41.184 [s, Leu $^{\beta}C$], 40.209 [s, Lys $^{\varepsilon}C$], 37.020 [s, Ile $^{\beta}C$], 31.844 [s, Lys $^{\delta}C$], 29.334 [s, Lys $^{\beta}C$], 25.377 [s, Ile $^{\gamma}CH$], 24.864 [s, Leu $^{\gamma}C$], 22.766 [s, Leu $^{\delta}C$], 22.274 [s, Lys $^{\gamma}C$], 21.809 [s, Leu $^{\delta}C$], 15.386, 11.254 [2s, Ile $^{\gamma}C$$H_3$ and $^{\delta}C$].

**Segment E (Z-Aib-Gly-Leu-Aib-O*t*Bu).** Overall yield: 71%. Melting point: 165–166 °C. $Rf_1$: 0.50, $Rf_2$: 0.80, $Rf_3$: 0.30. $[\alpha]_D^{20}$: –3.2° (*c* = 0.5, MeOH). IR (KBr): 3316, 1732, 1701, 1659, 1536 $cm^{-1}$. ESI-MS *m/z*: calculated for $C_{28}H_{44}N_4O_7$ 548.32, found 548.31. $^1H$ NMR (200 MHz, $CDCl_3$): $\delta$ 7.36 [m, 6H, Z phenyl CH, 1H NH], 6.93 [m, 1H, NH], 6.87 [s, 1H, Aib NH], 5.37 [s, 1H, Aib NH], 5.10 [2d, 2H, Z $CH_2$], 4.42 [m, 1H, Leu α-CH], 4.0–3.80 [m, 4H, Gly α-$CH_2$], 1.68 [m, 3H, Leu β-$CH_2$, Leu γ-CH], 1.49–1.51 [m, 12H, Aib 4 β-$CH_3$], 1.43 [s, 9H, O*t*Bu], 0.92 [m, 6H, Leu δ-$CH_3$]. $^{13}C$ NMR (100 MHz, $CDCl_3$): $\delta$ 174.893, 173.513, 171.315, 169.209 [4s, amide and ester *C*═O], 155.833 [s, urethane *C*═O], 135.528 [s, aromatic quaternary *C*], 128.137, 127.946 [2s, aromatic *C*], 80.824 [s, O*t*Bu quaternary *C*], 67.366 [s, urethane *C*$H_2$], 57.021, 51.930, 43.647 [3s, 4 $^{\alpha}C$], 39.849 [s, $^{\beta}C$], 27.751 [s, O*t*Bu *C*$H_3$], 24.782, 24.696, 24.617, 24.529, 24.350 [5s, Leu $^{\gamma}C$, Aib $^{\beta}C$], 22.853, 21.952 [2s, Leu $^{\delta}C$].

**Segment B-A (Z-Gly-Gly-Leu-Aib-Gly-Ile-Leu-OMe):[12].** Overall yield: 60%. Melting point: 152–153 °C. $Rf_1$: 0.40, $Rf_2$: 0.90, $Rf_3$: 0.10. $[\alpha]_D^{20}$: –39.1° (*c* = 0.5, MeOH). IR (KBr): 3318, 1734, 1706, 1651, 1540 $cm^{-1}$. ESI-MS *m/z*: calculated for $C_{37}H_{59}N_7O_{10}$ 761.43, found 761.43. $^1H$ NMR (400 MHz, $CDCl_3$): $\delta$ 8.19 [t, 1H, Gly NH], 7.68 [t, 1H, Gly NH], 7.59 [d, 1H, Ile NH], 7.45 [d, 1H, Leu NH], 7.35 [m, 5H, Z phenyl CH], 6.76 [m, 2H, Aib NH, Leu NH], 5.94 [t, 1H, Gly NH], 5.12 [m, 2H, Z

 

$CH_2$], 4.31–3.26 [m, 2H, Gly α-$CH_2$], 4.23 [m, 1H, Leu α-CH], 4.21–3.45 [m, 2H, Gly α-$CH_2$], 4.05 [m, 1H, Leu α-CH], 4.02 [m, 1H, Ile α-CH], 3.91 [m, 2H, Gly α-$CH_2$], 3.66 [s, 3H, OMe $CH_3$], 2.10 [m, 1H, Ile β-CH], 1.80–1.60 [m, 7H, Leu β-$CH_2$ and γ-CH, Ile 1 γ-CH], 1.57 [s, 3H, Aib β-$CH_3$], 1.44 [s, 3H, Aib β-$CH_3$], 1.13 [m, 1H, Ile 1 γ-CH], 1.00–0.80 [m, 18H, Leu δ-$CH_3$, Ile γ-$CH_3$ and δ-$CH_3$]. $^{13}$C NMR (150 MHz, $CDCl_3$): *δ* 174.743, 173.608, 173.483, 172.915, 171.949, 170.573, 170.398 [7s, ester and amide *C*═O], 157.586 [s, urethane *C*═O], 136.110 [s, aromatic quaternary *C*], 128.478, 128.160, 127.779 [3s, aromatic *C*], 67.230 [s, urethane *C*$H_2$], 58.378, 57.174, 53.749, 52.221, 51.951 [5s, $^{\alpha}$*C* and -O*C*$H_3$], 45.033, 43.387, 42.611 [3s, $^{\alpha}$*C* Gly], 40.036, 39.239, 35.376 [3s, Ile and Leu $^{\beta}$*C*], 24.834, 24.654, 24.607, 22.614, 22.467, 22.484, 21.549 [7s, Aib $^{\beta}$*C*, Ile $^{\gamma}$*C*H, Leu $^{\gamma}$*C* and $^{\delta}$*C*], 15.317, 10.632 [2s, Ile $^{\gamma}$*C*$H_3$ and $^{\delta}$*C*].

**Segment E-B [Z-Aib-Gly-Leu-Aib-Gly-Gly-Leu-Aib-O*t*Bu].** Overall yield: 61%. Melting point: 112–114 °C. $Rf_2$: 0.95, $Rf_3$: 0.20, $Rf_4$: 0.45. $[\alpha]_D^{20}$: −10.2° (*c* = 0.5, MeOH). IR (KBr): 3316, 1733, 1660, 1535 $cm^{-1}$. ESI-MS *m*/*z*: calculated for $C_{42}H_{68}N_8O_{11}$ 860.50, found 860.48. $^1$H NMR (400 MHz, $CDCl_3$): *δ* 7.90 [t, 1H, Gly NH], 7.81 [d, 1H, Leu NH], 7.52 [t, 1H, Gly NH], 7.49 [t, 1H, Gly NH], 7.35 [m, 5H, Z phenyl CH], 7.26 [s, 1H, Aib NH], 7.11 [d, 1H, Leu NH], 6.90 [s, 1H, Aib NH], 5.82 [s, 1H, Aib NH], 5.10 [m, 2H, Z $CH_2$], 4.38 [m, 1H, α-CH], 4.05 [m, 2H, 2 α-CH], 3.86 [m, 4H, 4 α-CH], 3.69 [m, 1H, α-CH], 1.72 [m, 6H, Leu β-$CH_2$ and γ-CH], 1.45 [m, 27H, O*t*Bu, Aib β-$CH_3$], 0.93 [m, 12H, Leu δ-$CH_3$]. $^{13}$C NMR (100 MHz, $CDCl_3$): *δ* 176.866, 174.689, 173.414, 172.198, 171.982, 171.081, 170.361 [7s, 8 amide and ester *C*═O], 156.593 [s, urethane *C*═O], 135.744 [s, aromatic quaternary *C*], 128.658, 128.339, 127.612 [3s, aromatic *C*], 80.842 [s, O*t*Bu quaternary *C*], 67.030 [s, urethane *C*$H_2$], 56.868, 56.570, 54.481, 52.511 [4s, 5 $^{\alpha}$*C* Leu and Aib],44.573, 44.454, 43.536 [3s, $^{\alpha}$*C* Gly], 40.191, 39.192 [2s, Leu $^{\beta}$*C*], 27.830 [s, O*t*Bu *C*$H_3$], 26.542, 26.248, 25.089, 24.803, 24.509, 24.376, 24.095 [7s, Leu $^{\gamma}$*C*, 6 Aib $^{\beta}$*C*], 23.860, 23.010, 21.357, 21.234 [4s, Leu $^{\delta}$*C*].

**K2-OMe**: Overall yield: 18%. Melting point: 148–150 °C. $Rf_2$: 0.70, $Rf_3$: 0.05, $Rf_4$: 0.05. $[\alpha]_D^{20}$: −24.8° (*c* = 0.2, MeOH). IR (KBr): 3321, 1743, 1655, 1538 $cm^{-1}$. ESI-MS *m*/*z*: calculated for $C_{57}H_{104}N_{12}O_{13}$ 1164.78, found 1164.81. $^1$H NMR (400 MHz, $H_2O/D_2O$ 9 : 1): *δ* 8.37 [m, 2H, 2 NH], 8.31 [s, 1H NH], 8.08 [t, 1H, NH], 7.96 [m, 2H, 2 NH], 7.85 [s, 1H, 1 NH], 7.80–7.77 [m, 2H, 2 NH], 7.64–7.60 [m, 2H 2 NH], 7.48 [bs, 1H], 4.36 [m, 1H], 4.20–3.68 [m, 10H 10 α-CH], 3.64 [s, 3H, OMe $CH_3$], 3.11 [m, 2H, Lys$^2$ ε-$CH_2$], 2.23–2.11 [m, 2H, *n*Oct $CH_2$], 1.98–1.51 [m, 30H], 1.39, 1.37. 1.35, 1.33, 1.32, [5s, 18H, β-$CH_3$ Aib], 1.20–1.03 [m, 11H], 0.83–0.70 [m, 24H, δ-$CH_3$ Leu, δ-$CH_3$ and γ-$CH_3$ Ile], 0.69–0.65 [t, 2H, *n*Oct $CH_3$]. $^{13}$C NMR (100 MHz, $H_2O/D_2O$ 9 : 1): *δ* 183.497, 177.329, 175.247, 175.103, 173.887, 173.689, 173.626, 173.401, 173.095, 173.043, 172.158, 172.040 [12s, ester and amide *C*═O], 56.751, 56.461, 56.372, 55.248, 53.381, 52.732, 51.458, 50.908, 49.247 [9s, $^{\alpha}$*C* and -O*C*$H_3$], 44.486, 43.462, 42.645 [3s, $^{\alpha}$*C* Gly], 39.429, 36.401, 35.347, 31.439 [4s, *n*-Oct, Lys $^{\varepsilon}$*C* and $^{\delta}$*C*, Ile and Leu $^{\beta}$*C*], 29.585, 28.986, 28.781, 26.327, 25.212, 25.093, 24.761, 24.541, 24.105, 23.538, 23.211, 22.803, 22.667, 22.574, 22.471, 22.342, 21.212, 20.942, 20.575 [19s, *n*-Oct, Lys $^{\gamma}$*C* and $^{\beta}$*C*, Aib $^{\beta}$*C*, Ile $^{\gamma}$*C*H, Leu $^{\gamma}$*C* and $^{\delta}$*C*], 14.975, 13.634, 11.044 [3s, *n*-Oct, Ile $^{\gamma}$*C*$H_3$ and $^{\delta}$*C*].

**K9-OMe**: Overall yield: 25%. Melting point: 152–153 °C. $Rf_2$: 0.70, $Rf_3$: 0.05 $Rf_4$: 0.05. $[\alpha]_D^{20}$: −14.6° (*c* = 0.2, MeOH). IR (KBr): 3317, 1743, 1657, 1537 $cm^{-1}$. ESI *m*/*z*: calculated for $C_{57}H_{104}N_{12}O_{13}$ 1164.78, found 1164.82. $^1$H NMR (600 MHz, $H_2O/D_2O$ 9 : 1): *δ* 8.66 [t, 1H, Gly$^2$ NH], 8.43 [t, 1H, Gly$^5$-NH], 8.35 [s, 1H, Aib$^1$-NH], 8.08 [t, 1H, Gly$^6$-NH], 8.04 [d, 1H, Leu$^3$-NH], 7.85 [d, 1H, Leu$^7$-NH], 7.84 [s, 1H, Aib$^8$-NH], 7.82 [s, 1H, Aib$^4$-NH], 7.60–7.59 [d, 1H, Ile$^{10}$ NH], 7.55 [d, 1H, Leu$^{11}$-NH], 7.37 [d, 1H, Lys$^9$ NH], 4.36 [m, 1H, Leu$^{11}$ α-CH], 4.20 [m, 1H, Leu$^3$ α-CH], 4.13–4.12 [m, 2H, Ile$^{10}$ α-CH and Lys$^9$ α-CH], 4.04 [m, 1H, Leu$^7$ α-CH], 3.96 [m, 1H, Gly$^6$ 1 α-CH], 3.92 [m, 1H], 3.89 [m, 1H, Gly$^2$ 1 α-CH], 3.84 [m, 1H, Gly$^5$ 1 α-CH], 3.76–3.71 [m, 3H, Gly$^5$ α-CH, Gly$^6$ α-CH and Gly$^2$ α-CH], 3.65 [s, 3H, OMe $CH_3$], 2.92 [m, 2H, Lys$^9$ ε-$CH_2$], 2.17 [m, 2H, *n*Oct $CH_2$], 1.85 [m, 1H, Ile$^{10}$ β-CH], 1.74 [m, 2H, Lys$^9$ β-$CH_2$], 1.68 [m, 2H, Leu$^3$ β-$CH_2$], 1.61 [m, 2H, Leu$^{11}$ β-$CH_2$], 1.55 [m, 1H, Leu$^3$ 1 γ-CH], 1.44 [m, 2H, *n*Oct β-$CH_2$], 1.42 [s, 8H, Lys$^9$ γ-$CH_2$, Ile$^{10}$ 1 γ-CH and Aib$^4$ β-$CH_3$], 1.36 [s, 6H, Aib$^1$ 2 β-$CH_3$], 1.35 and 1.32 [2s, 6H, 2 Aib$^8$ β-$CH_3$], 1.20–1.04 [m, 11H, Ile$^{10}$ 1 γ-CH and *n*Oct $(CH_2)_5$], 0.83–0.79 [m, 9H, Leu$^3$ 2 δ-$CH_3$, Ile$^{10}$ γ-$CH_3$], 0.76–0.72 [m, 15H, Leu$^7$ 2 δ-$CH_3$, Ile$^{10}$ δ-$CH_3$ and Leu$^{11}$ 2 δ-$CH_3$], 0.67 [t, 2H, *n*Oct $CH_3$]. $^{13}$C NMR (150 MHz, $H_2O/D_2O$ 9 : 1): *δ* 190.053, 178.580, 175.148, 175.088, 174.851, 174.782, 174.693, 174.276, 174.248, 174.216, 173.528, 173.490 [12s, ester and amide *C*═O], 56.777, 56.398, 56.308, 54.828, 54.132, 53.504, 53.080, 52.781, 50.754 [9s, $^{\alpha}$*C* and -O*C*$H_3$], 44.062, 43.775, 42.912 [3s, $^{\alpha}$*C* Gly], 39.447, 36.507, 35.279, 31.463 [4s, *n*-Oct, Lys $^{\varepsilon}$*C* and $^{\delta}$*C*, Ile and Leu $^{\beta}$*C*], 29.044, 28.826, 26.320, 25.839, 25.220, 25.163, 25.037, 24.392, 24.067, 23.624, 23.598, 22.925, 22.832, 22.585, 22.368, 22.321, 21.349, 21.126, 20.484 [19s, *n*-Oct, Lys $^{\gamma}$*C* and $^{\beta}$*C*, Aib $^{\beta}$*C*, Ile $^{\gamma}$*C*H, Leu $^{\gamma}$*C* and $^{\delta}$*C*], 15.122, 15.060, 13.641, 11.062 [4s, *n*-Oct, Ile $^{\gamma}$*C*$H_3$ and $^{\delta}$*C*].

**Solid-phase peptide synthesis.** Assembly of peptides on the Advanced ChemTech (Louisville, KY) 348Ω peptide synthesizer was performed on a 0.05 mmol scale by the FastMoc methodology, as described below, starting with the Lol-substituted 2-chlorotrityl resin[51,52] (Iris Biotech, Marktredwitz, Germany) (110 mg, checked loading 0.40 mmol $g^{-1}$). The Lys side chain was protected with the Boc group, while the removal of the N$^{\alpha}$-Fmoc protection was performed with 20% piperidine in *N*,*N*-dimethylformamide. The total syntheses were achieved by using the very efficient HATU [2-(1*H*-7-aza-1,2,3-benzotriazol-1-yl)-1,1,3,3-tetramethyl uronium hexafluorophosphate][74] double coupling C-activation procedure for the formation of peptide bonds involving the three poorly reactive Aib[49] residues in the native sequence. All other coupling reactions were conducted using the HBTU [2-(1*H*-1,2,3-benzotriazol-1-yl)-1,1,3,3-tetramethyl uronium hexafluorophosphate]/HOBt procedure[76] for activation of the carboxylic function. Each coupling step was carried out by use of a threefold excess of the Fmoc N$^{\alpha}$-protected α-amino acid in the presence of a sevenfold excess of *N*,*N*′-diisopropylethylamine for 60 min. Final on-resin N$^{\alpha}$-*n*-octanoylation was achieved using a threefold excess of *n*-Oct-OH preactivated with EDC/HOAt[74] in the presence of *N*-methylmorpholine. Cleavage of the peptide from 2-chlorotrityl resin was performed by repeated treatments with 30% HFIP (1,1,1,3,3,3,-hexafluoropropan-2-ol) in distilled $CH_2Cl_2$ (45 min each).[52] The peptide cleaved from the resin was filtered off and collected. Then, the solution was concentrated under a flow of nitrogen. The crude peptides, protected as Boc

derivatives at side-chain of Lys residues, were purified by flash chromatography using chloroform-methanol (13 : 1) mixture as eluant. The purified fractions were subjected to Boc removal using 3 M HCl in methanol, yielding (without further purification steps) the desired products in a >98% purity (Fig. 1).

**TRIC** ESI-MS *m/z*: calculated for $C_{52}H_{95}N_{11}O_{12}$ 1065.72, found 1065.75

**K5** ESI-MS *m/z*: calculated for $C_{56}H_{104}N_{12}O_{12}$ 1136.79, found 1136.77

**K6** ESI-MS *m/z*: calculated for $C_{56}H_{104}N_{12}O_{12}$ 1136.79, found 1136.86

**K56** ESI-MS *m/z*: calculated for $C_{60}H_{113}N_{13}O_{12}$ 1207.86, found 1207.86

**K259U6** ESI-MS *m/z*: calculated for $C_{66}H_{126}N_{14}O_{12}$ 1306.97, found 1306.95

**K2569** ESI-MS *m/z*: calculated for $C_{68}H_{131}N_{15}O_{12}$ 1350.01, found 1350.00

### FT-IR absorption

The FT-IR absorption spectra were recorded at 293 K using a Perkin-Elmer model 1720X FT-IR spectrophotometer, nitrogen flushed, equipped with a sample-shuttle device, at 2 $cm^{-1}$ nominal resolution, averaging 100 scans. Solvent (baseline) spectra were recorded under the same conditions. For spectral elaboration, the software SPECTRACALC provided by Galactic (Salem, MA) was employed. Cells with path lengths of 1.0 and 10 mm (with $CaF_2$ windows) were used. Spectrograde deuterated chloroform (99.8%, *d*) was purchased from Merck (Darmstadt, Germany).

### Circular dichroism

The CD spectra were measured on a Jasco (Tokyo, Japan) model J-715 spectropolarimeter equipped with a Haake thermostat (Thermo Fisher Scientific, Waltham, MA). Baselines were corrected by subtracting the solvent contribution. Fused quartz cells of 1.0 mm and 10.0 mm path lengths (Hellma, Mühlheim, Germany) were used. The values are expressed in terms of $[\theta]_T$, the total molar ellipticity (deg × $cm^2$ x $dmol^{-1}$). Spectrograde methanol 99.9% (Acros Organic, Geel, Belgium) was used as solvent.

### Nuclear magnetic resonance

All $^1H$ NMR and $^{13}C$ NMR experiments were performed on a Bruker AVANCE DMX-600, DRX-400 or AC200 spectrometer operating at 600 MHz, 400 MHz or 200 MHz, respectively, using the TOPSPIN software package. For the characterizations, the solvent was used as the internal standard: $CDCl_3$ ($^1H$: $\delta$ = 7.26 ppm; $^{13}C$: $\delta$ = 77.00 ppm). Splitting patterns are abbreviated as follows: (s) singlet, (d) doublet, (t) triplet, (q) quartet, (m) multiplet. Samples for NMR conformational studies were dissolved in water (9 : 1 $H_2O/D_2O$), in water (9 : 1 $H_2O/D_2O$) containing SDS-$d_{25}$ (100 mM) or in MeOH-$d_3$ solution (peptide concentrations: 1.8 mM, 3.5 mM and 5.6 mM, respectively). The pH of the SDS-containing solution was adjusted at 2.83 by adding 1 μl of 3 M HCl. The spectra were recorded at 313 K. Presaturation of the $H_2O$ solvent signal was obtained using a WATERGATE gradient program. All homonuclear spectra were acquired by collecting 512 experiments, each one consisting of 64–80 scans and 2 K data points. The spin systems of protein amino acid residues were identified using standard DQF-COSY[77] and CLEAN-TOCSY[78,79] spectra. In the latter case, the spin-lock pulse sequence was 70 ms long. The assignment of the two methyl groups belonging to the same Aib residue was obtained by means of $^1H$-$^{13}C$ 2D correlation spectra. To optimize the digital resolution in the carbon dimension, heteronuclear multiple quantum coherence (HMQC[80]) and heteronuclear multiple bond coherence (HMBC[81]) experiments were acquired using selective excitation by means of Gaussian-shaped pulses with 1% truncation.[82,83]

The $C^\beta$-selective HMQC experiments with gradient coherence selection[84] were recorded with 320 $t_1$ increments, of 300 scans and 2 K points each.[80] A spectral width of 16 ppm centered at 22 ppm in F1 was used, yielding a digital resolution of 2.36 Hz/pt prior to zero filling. HMBC experiments with selective excitation in the CO region were performed using a long-range coupling constant of 7.5 Hz, a spectral width in F1 of 15 ppm centered at 176 ppm, 250 $t_1$ experiments of 640 scans, and 4 K points in F2. The digital resolution in F1, prior to zero filling, was 2.2 Hz/pt. NOESY experiments were used for sequence specific assignment.

### Proteolytic stability

To evaluate their proteolytic stability, the peptides were dissolved in a buffer solution (50 mM Tris·HCl, pH 7.8). The enzymes trypsin, pepsin, chymotrypsin, endoprotease Glu-c V8, pronase E, a protease from *Streptomyces griseus*, elastase (from porcine pancreas), and subtilisin A (from *Bacillus sp.*) were obtained from Sigma (St. Louis, MO). The enzyme was added to the peptide in the ratio 1 : 100 (*w*/*w*) and the mixture was incubated at 37° C for 4 h. The samples were analyzed using a $C_{18}$ reverse-phase HPLC column. Appropriate programmed gradients from 40 to 95% B solution for 20 or 50 min were applied using eluants A ($H_2O$/0.05% TFA) and B ($CH_3CN$/0.075% TFA).

### SUV preparation

DOPC was purchased from Avanti Polar Lipids, Inc. (Alabaster, AL), while Ch was a Sigma-Aldrich (St. Louis, MO) product. The lipid mixture, DOPC/Ch (7 : 3) was dissolved in $CHCl_3$ in a test tube, dried under $N_2$, and lyophilized overnight. The lipid film was reconstituted with a solution of CF in 30 mM Hepes buffer (pH 7.4) at room temperature for 1 h. To make SUVs, the resulting multilamellar vesicle suspension was sonicated (GEX 400 Ultrasonic Processor, Sigma) on ice until the initially cloudy lipid dispersion became translucent. The excess of fluorescent dye was eliminated by gel filtration on Sephadex G-75 (Sigma). SUVs were diluted to a concentration of 0.06 mM with Hepes buffer (5 mm Hepes, 100 mM NaCl, pH 7.4). The SUVs were stored at 4 °C and used within 24 h.

### Leakage from lipid vesicles

The peptide-induced leakage from SUVs was measured at 293 K using the CF-entrapped vesicle technique[85] and a Perkin Elmer model MPF-66 spectrofluorimeter. The SUVs composition used was DOPC/CH 7 : 3. SUVs were prepared as described above. The phospholipid concentration was kept constant (0.06 mM), and increasing [peptide]/[lipid] molar ratios ($R^{-1}$) were obtained by adding aliquots of water solutions of peptides, except for the native non hydrosoluble trichogin GA IV, used as reference compound,

 

which was added as a methanol solution, keeping the final MeOH concentration below 5% by volume. After rapid and vigorous stirring, the time course of fluorescence change corresponding to CF escape was recorded at 520 nm (6-nm band pass) with $\lambda_{exc}$ 488 nm (3-nm band pass). The percentage of released CF at time $t$ was determined as $(F_t-F_0)/(F_T-F_0)$ x 100, with $F_0$ = fluorescence intensity of vesicles in the absence of peptide, $F_t$ = fluorescence intensity of vesicles at time $t$ in the presence of peptide, and $F_T$ = total fluorescence intensity determined by disrupting the vesicles by addition of 50 µL of a Triton X-100 solution. The kinetics experiments were stopped at 20 min.

### Membrane depolarization assay

The peptide ability to dissipate the membrane potential was determined using intact *S. aureus*, *E. coli*, and the membrane potential-sensitive, fluorescent dye 3,3′-dipropylthiadicarbocyanine iodide [$DiSC_3$-5, from Molecular Probes (Eugene, OR)]. *S. aureus* and *E. coli* bacteria were grown to mid-logarithmic phase at 37 °C. The cells were washed three times in buffer A (20 mM glucose, 5 mM Hepes, pH 7.2) and resuspended to an $OD_{600\,nm}$ of 0.05 in buffer A containing 0.1 M KCl. The cells were then incubated with $DiSC_3$-5 (final concentration 0.5 µM) until stable baseline fluorescence was achieved (*ca.* 60 min). The experiments were conducted in sterile 96-well plates at a final volume of 200 µl. Then, the peptides dissolved in buffer A were added to achieve the desired concentration. Membrane depolarization was detected as an increase in the $DiSC_3$-5 fluorescence (excitation wavelength, 622 nm; emission wavelength, 670 nm).[86]

### Bacterial strains

*Escherichia coli* (ATCC 25 922), *Listeria monocytogenes* (ATCC 19 115), and *Staphylococcus aureus* (ATCC 25 923) were obtained from American Type Culture Collection. *Bacillus subtilis* (KCTC 1918), *Staphylococcus epidermidis* (KCTC 3096), and *Pseudomonas aeruginosa* (KCTC 1637) were from the Korean Collection for Type Cultures (KCTC), Korean Research Institute of Bioscience and Biotechnology (KRIBB), Taejon, Korea. To assess the antimicrobial activities of our peptides against antibiotic-resistant bacteria, clinically isolated multidrug-resistant bacterial strains were obtained from the Culture Collection of Antibiotic-Resistant Microbes (CCARM) at Seoul Women's University, Korea. These included five strains of methicillin-resistant *S. aureus* (MRSA) (CCARM 3089, CCARM 3090, CCARM 3108, CCARM 3114, and CCARM 3126).

### Antibacterial activity

To determine the MIC values for the tested peptides, serial microdilution assays were performed. Cells were grown to log-phase in 10 g $l^{-1}$ bactotryptone, 5 g $l^{-1}$ yeast extract, and 10 g $l^{-1}$ NaCl, pH 7.0, then passed through a 0.22 µm filter and stepwise-diluted in a medium of 1% bactopeptone. Each organism to be tested was suspended at $2 \times 10^6$ colony formation units (CFU) $ml^{-1}$ in growth medium. A stock solution of each peptide was prepared by dissolving it in the minimum amount of dimethylsulfoxide (DMSO) and diluting with PBS (phosphate buffered saline). The maximum amount of DMSO in each solution was 1.45%. Then, eight solutions, obtained by successive two-fold dilutions, were prepared and tested by mixing 100 µl of each solution with 100 µl of the organism suspension in a microtiter plate well. The test for each peptide was repeated three times at every concentration. The plates were incubated for 18 h at 37 °C. The MIC value was defined as the lowest concentration of peptide that gave no visible growth on the plate. The endpoint was detected by use of a spectrophotometer.

### Hemolytic activity

The hemolytic activity of each peptide was determined using hRBCs from healthy donors that were collected on heparin. Fresh hRBCs were washed three times in PBS (phosphate buffered saline) by centrifugation for 10 min at 800× g and resuspension in PBS. The peptides dissolved in PBS were then added to 100 µL of stock hRBCs suspended in PBS (final hRBCs concentration: 8%, v/v). The samples were incubated with agitation for 1 h at 37 °C and centrifuged at 800×g for 10 min. The absorbance of the supernatant was measured at 414 nm. Controls for zero hemolysis (blank) and 100% hemolysis consisted of hRBCs suspended in PBS and 1% Triton X-100, respectively. The percentage hemolysis was calculated using the following equation:% hemolysis = [($A_{414\,nm}$ with protein solution- $A_{414\,nm}$ in PBS)/($A_{414\,nm}$ with 0.1% Triton X-100- $A_{414\,nm}$ in PBS)] x 100. Each measurement was made in triplicate.[87,88] The hemolytic peptide melittin was synthesized in the Chosun University laboratories.

### Cytotoxicity

HaCaT (Human adult low-Calcium high Temperature keratinocyte cells) were cultivated in Dulbeccos's Minimal Eale Medium (DMEM) at 37 °C and 5% $CO_2$ for 5–7 days. Assays were performed by incubation of $2 \times 10^3$ cells with various concentrations of peptide for 19 h at 37 °C and 5% $CO_2$ in a 96-well plate. The Triton X-100 (0.1% final concentration) was used as negative control and pure medium assay was used as positive control. Proliferation and viability were determined by MTT [3-(4,5-dimethyl-2-thiazolyl)-2,5-diphenyl tetrazolium bromide] assay. The plate was then incubated for 24 h before adding to each well 50 µl of MTT solution. The medium containing MTT was removed and 100 µl of DMSO were added. Cells were incubated for 10 min at 37 °C under gentle shaking. The optical density was read at 550 nm in an enzyme-linked immunosorbent assay plate reader after 2 h of incubation. Cell viability was determined relative to the control. Studies were performed in triplicate.

### Antifungal activity

Microdilution assays were performed to establish the MIC values for the peptides. *Candida albicans* was grown at 28 °C in YPD (2% dextrose, 1% peptone, and 0.5% yeast extract, pH 5.5) for 3 h. Cell densities were counted with a hemocytometer. The fungal cells ($2 \times 10^3$/well) were seeded on the wells of a flat-bottom 96-well microtiter plate (Greiner, Nurtingen,Germany) containing YPD (100 µl/well). Serial dilutions of the peptide solution were added to each well, and the cell suspension was incubated at 28 °C for 24 h. A 10 µl of MTT solution (5 mg $ml^{-1}$) was added to each well, and the plates were incubated at 37 °C for 4 h. Then, absorbance at 570 nm was measured using an Emax microtiter plate reader (Molecular

Devices, California, USA). All assays were performed in triplicate. The assays for antifungal activity against *Fusarium oxysporum*, *Rhizoctonia solani*, *Aspergillus awamori*, *Aspergillus parasiticus*, and *Astragalus flavus* were carried out in 100 × 15 mm Petri dishes containing YPD. After the mycelial colony had developed, sterile blank paper disks (8 mm diameter) were placed 5 mm from the leading edge of the mycelial colony. An aliquot of the peptide test sample in 2-(*N*-morpholino)ethanesulfonic acid (MES) buffer (20 mM, pH 6.0) was added to each disk, and the plates were incubated at 28 °C for 72 h. Antifungal activity was shown as a clear zone of growth inhibition.

## References


1 R. M. Epand and R. F. Epand, *J. Pept. Sci.*, 2011, **17**, 298–305.
2 H. Duclohier, *Curr. Pharm. Des.*, 2010, **16**, 3212–3223.
3 R. E. W. Hancock and H.-G. Sahl, *Nat. Biotechnol.*, 2006, **24**, 1551–1557.
4 C. Toniolo and H. Brückner, *Peptaibiotics*, Wiley/VCH, Weinheim/Zürich, 2009.
5 C. Toniolo, M. Crisma, F. Formaggio, C. Peggion, R. F. Epand and R. M. Epand, *Cell. Mol. Life Sci.*, 2001, **58**, 1179–1188.
6 C. Peggion, F. Formaggio, M. Crisma, R. F. Epand, R. M. Epand and C. Toniolo, *J. Pept. Sci.*, 2003, **9**, 679–689.
7 C. Auvin-Guette, S. Rebuffat, Y. Prigent and B. Bodo, *J. Am. Chem. Soc.*, 1992, **114**, 2170–2174.
8 S. Rebuffat, C. Goulard, B. Bodo and M.-F. Roquebert, *Recent Res. Devel. Org. Biorg. Chem.*, 1999, **3**, 65–91.
9 C. Toniolo, C. Peggion, M. Crisma, F. Formaggio, X. Shui and D. S. Eggleston, *Nat. Struct. Biol.*, 1994, **1**, 908–914.
10 R. Gurunath and P. Balaram, *Biopolymers*, 1995, **35**, 21–29.
11 V. Monaco, F. Formaggio, M. Crisma, C. Toniolo, X. Shui and D. S. Eggleston, *Biopolymers*, 1996, **39**, 31–42.
12 C. Toniolo, M. Crisma, F. Formaggio, C. Peggion, V. Monaco, C. Goulard, S. Rebuffat and B. Bodo, *J. Am. Chem. Soc.*, 1996, **118**, 4952–4958.
13 P. Scrimin, A. Veronese, P. Tecilla, U. Tonellato, V. Monaco, F. Formaggio, M. Crisma and C. Toniolo, *J. Am. Chem. Soc.*, 1996, **118**, 2505–2506.
14 M. Crisma, V. Monaco, F. Formaggio, C. Toniolo, C. George and J. L. Flippen-Anderson, *Lett. Pept. Sci.*, 1997, **4**, 213–218.
15 V. Monaco, E. Locardi, F. Formaggio, M. Crisma, S. Mammi, E. Peggion, C. Toniolo, S. Rebuffat and B. Bodo, *J. Pept. Res.*, 2009, **52**, 261–272.
16 E. Locardi, S. Mammi, E. Peggion, V. Monaco, F. Formaggio, M. Crisma, C. Toniolo, B. Bodo, S. Rebuffat, J. Kamphuis and Q. B. Broxterman, *J. Pept. Sci.*, 1998, **4**, 389–399.
17 C. Peggion, V. Moretto, F. Formaggio, M. Crisma, C. Toniolo, J. Kamphuis, B. Kaptein and Q. B. Broxterman, *J. Pept. Res.*, 2001, **58**, 317–324.
18 F. Formaggio, C. Peggion, M. Crisma and C. Toniolo, *J. Chem. Soc., Perkin Trans. 2*, 2001, 1372–1377.
19 M. Saviano, R. Improta, E. Benedetti, B. Carrozzini, G. L. Cascarano, C. Didierjean, C. Toniolo and M. Crisma, *ChemBioChem*, 2004, **5**, 541–544.
20 I. L. Karle and P. Balaram, *Biochemistry*, 1990, **29**, 6747–6756.
21 E. Benedetti, B. Di Blasio, V. Pavone, C. Pedone, C. Toniolo and M. Crisma, *Biopolymers*, 1992, **32**, 453–456.
22 C. Toniolo, M. Crisma, F. Formaggio, G. Valle, G. Cavicchioni, G. Précigoux, A. Aubry and J. Kamphuis, *Biopolymers*, 1993, **33**, 1061–1072.
23 C. Toniolo, M. Crisma and F. Formaggio, *Biopolymers*, 2001, **60**, 396–419.
24 C. Toniolo and E. Benedetti, *Trends Biochem. Sci.*, 1991, **16**, 350–353.
25 K. A. Bolin and G. L. Millhauser, *Acc. Chem. Res.*, 1999, **32**, 1027–1033.
26 V. Monaco, F. Formaggio, M. Crisma, C. Toniolo, P. Hanson, G. Millhauser, C. George, J. R. Deschamps and J. L. Flippen-Anderson, *Bioorg. Med. Chem.*, 1999, **7**, 119–131.
27 D. J. Anderson, P. Hanson, J. Mc Nulty, G. Millhauser, V. Monaco, F. Formaggio, M. Crisma and C. Toniolo, *J. Am. Chem. Soc.*, 1999, **121**, 6919–6927.
28 V. Monaco, F. Formaggio, M. Crisma, C. Toniolo, P. Hanson and G. L. Millhauser, *Biopolymers*, 1999, **50**, 239–253.
29 A. D. Milov, Yu. D. Tsvetkov, F. Formaggio, M. Crisma, C. Toniolo and J. Raap, *J. Am. Chem. Soc.*, 2001, **123**, 3784–3789.
30 A. D. Milov, Yu. D. Tsvetkov, F. Formaggio, M. Crisma, C. Toniolo, G. L. Millhauser and J. Raap, *J. Phys. Chem. B*, 2001, **105**, 11206–11213.
31 A. D. Milov, Yu. D. Tsvetkov, F. Formaggio, S. Oancea, C. Toniolo and J. Raap, *J. Phys. Chem. B*, 2003, **107**, 13719–13727.
32 A. D. Milov, Yu. D. Tsvetkov, F. Formaggio, M. Crisma, C. Toniolo and J. Raap, *J. Pept. Sci.*, 2003, **9**, 690–700.
33 A. D. Milov, Yu. D. Tsvetkov, F. Formaggio, S. Oancea, C. Toniolo and J. Raap, *Phys. Chem. Chem. Phys.*, 2004, **6**, 3596–3603.
34 L. Stella, C. Mazzuca, M. Venanzi, A. Palleschi, M. Didonè, F. Formaggio, C. Toniolo and B. Pispisa, *Biophys. J.*, 2004, **86**, 936–945.
35 A. D. Milov, D. A. Erilov, E. S. Salnikov, Yu. D. Tsvetkov, F. Formaggio, C. Toniolo and J. Raap, *Phys. Chem. Chem. Phys.*, 2005, **7**, 1794–1799.
36 C. Mazzuca, L. Stella, M. Venanzi, F. Formaggio, C. Toniolo and B. Pispisa, *Biophys. J.*, 2005, **88**, 3411–3421.
37 E. S. Salnikov, D. A. Erilov, A. D. Milov, Yu. D. Tsvetkov, C. Peggion, F. Formaggio, C. Toniolo, J. Raap and S. A. Dzuba, *Biophys. J.*, 2006, **91**, 1532–1540.
38 M. Venanzi, E. Gatto, G. Bocchinfuso, A. Palleschi, L. Stella, F. Formaggio and C. Toniolo, *ChemBioChem*, 2006, **7**, 43–45.
39 E. Gatto, C. Mazzuca, L. Stella, M. Venanzi, C. Toniolo and B. Pispisa, *J. Phys. Chem. B*, 2006, **110**, 22813–22818.
40 M. Venanzi, E. Gatto, G. Bocchinfuso, A. Palleschi, L. Stella, C. Baldini, F. Formaggio and C. Toniolo, *J. Phys. Chem. B*, 2006, **110**, 22834–22841.
41 M. Venanzi, G. Bocchinfuso, E. Gatto, A. Palleschi, L. Stella, F. Formaggio and C. Toniolo, *ChemBioChem*, 2009, **10**, 91–97.
42 V. N. Syryamina, N. P. Isaev, C. Peggion, F. Formaggio, C. Toniolo, J. Raap and S. A. Dzuba, *J. Phys. Chem. B*, 2010, **114**, 12277–12283.
43 C. Mazzuca, B. Orioni, M. Coletta, F. Formaggio, C. Toniolo, G. Maulucci, M. De Spirito, B. Pispisa, M. Venanzi and L. Stella, *Biophys. J.*, 2010, **99**, 1791–1800.
44 S. Smeazzetto, M. De Zotti and M. R. Moncelli, *Electrochem. Commun.*, 2011, **13**, 834–836.
45 C. Heuber, F. Formaggio, C. Baldini, C. Toniolo and K. Müller, *Chem. Biodiversity*, 2007, **4**, 1200–1217.
46 R. F. Epand, R. M. Epand, V. Monaco, S. Stoia, F. Formaggio, M. Crisma and C. Toniolo, *Eur. J. Biochem.*, 1999, **266**, 1021–1028.
47 R. F. Epand, R. M. Epand, F. Formaggio, M. Crisma, H. Wu, R. I. Lehrer and C. Toniolo, *Eur. J. Biochem.*, 2001, **268**, 703–712.
48 M. De Zotti, B. Biondi, F. Formaggio, C. Toniolo, L. Stella, Y. Park and K.-S. Hahm, *J. Pept. Sci.*, 2009, **15**, 615–619.
49 F. Formaggio, Q. B. Broxterman and C. Toniolo, in *Houben-Weyl: Methods of Organic Chemistry, Synthesis of Peptides and Peptidomimetics*, Vol. E22c, ed. M. Goodman, A. Felix, L. Moroder and C. Toniolo, Thieme, Stuttgart, Germany, 2003, pp. 292–310.
50 M. De Zotti, B. Biondi, C. Peggion, Y. Park, K.-S. Hahm, F. Formaggio and C. Toniolo, *J. Pept. Sci.*, 2011, **17**, 585–594.
51 K. Barlos, O. Chatzi, D. Gatos and G. Stavropoulos, *Int. J. Pept. Protein Res.*, 1991, **37**, 513–520.
52 R. Bollhagen, M. Schmiedberger, K. Barlos and E. Grell, *J. Chem. Soc., Chem. Commun.*, 1994, 2559–2560.
53 C. U. Hjørringgaard, J. M. Pedersen, T. Vosegaard, N. C. Nielsen and T. Skrydstrup, *J. Org. Chem.*, 2009, **74**, 1329–1332.
54 L. J. Bellamy, *The Infrared Spectra of Complex Molecules*, 2nd edn, Methuen, London, 1966.
55 M. T. Cung, M. Marraud and J. Néel, *Ann. Chim. (Paris)*, 1972, 183–209.
56 E. S. Pysh and C. Toniolo, *J. Am. Chem. Soc.*, 1977, **99**, 6211–6219.
57 S. Beychok, in *Poly-α-Amino Acids: Protein Models for Conformational Studies*, ed. G. D. Fasman, Dekker, New York, 1967, pp. 293–337.
58 M. C. Manning and R. W. Woody, *Biopolymers*, 1991, **31**, 569–585.
59 C. Toniolo, A. Polese, F. Formaggio, M. Crisma and J. Kamphuis, *J. Am. Chem. Soc.*, 1996, **118**, 2744–2745.
60 F. Formaggio, M. Crisma, P. Rossi, P. Scrimin, B. Kaptein, Q. B. Broxterman, J. Kamphuis and C. Toniolo, *Chem.–Eur. J.*, 2006, **6**, 4498–4504.
61 P. M. Hardy, in *Chemistry and Biochemistry of the Amino Acids*; ed. G. C. Barrett, Chapman and Hall, London, 1985, pp. 6–24.
62 I. André, S. Linse and F. A. A. Mulder, *J. Am. Chem. Soc.*, 2007, **129**, 15805–15813.




 

63 K. Wüthrich, *NMR of Proteins and Nucleic Acids*, Wiley, New York, 1986.
64 G. Irmscher and G. Jung, *Eur. J. Biochem.*, 1977, **80**, 165–174.
65 H.-H. Nguyen, D. Imhof, M. Kronen, B. Schlegel, A. Hartl, U. Gräfe, L. Gera and S. Reissmann, *J. Med. Chem.*, 2002, **45**, 2781–2787.
66 R. Banerjee, G. Basu, P. Chène and S. Roy, *J. Pept. Res.*, 2002, **60**, 88–94.
67 H. Yamaguchi, H. Kodama, S. Osada, F. Kato, M. Jelokhani-Niaraki and M. Kondo, *Biosci. Biotechnol. Biochem.*, 2003, **67**, 2269–2272.
68 S. Zikou, A.-I. Koukkou, P. Mastora, M. Sakarellos-Daitsiotis, C. Sakarellos, C. Drainas and E. Panou-Pomonis, *J. Pept. Sci.*, 2007, **13**, 481–486.
69 J. D. Sadowsky, J. K. Murray, Y. Tomita and S. H. Gellman, *ChemBioChem*, 2007, **8**, 903–916.
70 J. Svenson, W. Stensen, B.-O. Brandsdal, B. E. Haug, J. Monrad and J. S. Svendsen, *Biochemistry*, 2008, **47**, 3777–3788.
71 L. P. Miranda, K. A. Winters, C. V. Gegg, A. Patel, J. Aral, J. Long, J. Zhang, S. Diamond, M. Guido, S. Stanislaus, M. Ma, H. Li, M. J. Rose, L. Poppe and M. M. Véniant, *J. Med. Chem.*, 2008, **51**, 2758–2765.
72 J. Taira, Y. Kida, H. Yamaguchi, K. Kuwano, Y. Higashimoto and H. Kodama, *J. Pept. Sci.*, 2010, **16**, 607–612.
73 B. L. Feringa, *Molecular Switches*, Wiley-VCH, Weinheim, Germany, 2003.
74 L. A. Carpino, *J. Am. Chem. Soc.*, 1993, **115**, 4397–4398.
75 W. König and R. Geiger, *Chem. Ber.*, 1970, **103**, 788–798.
76 L. A. Carpino, A. El-Faham, C. A. Minor and F. Albericio, *J. Chem. Soc. Chem. Commun.*, 1994, 201–203.
77 M. Rance, O. W. Sørensen, G. Bodenhausen, G. Wagner, R. R. Ernst and K. Wüthrich, *Biochem. Biophys. Res. Commun.*, 1983, **117**, 479–485.
78 A. Bax and D. G. Davis, *J. Magn. Reson.*, 1985, **65**, 355–360.
79 C. Griesinger, G. Otting, K. Wüthrich and R. R. Ernst, *J. Am. Chem. Soc.*, 1988, **110**, 7870–7872.
80 A. Bax and S. Subramanian, *J. Magn. Reson.*, 1986, **67**, 565–569.
81 A. Bax and M. F. Summers, *J. Am. Chem. Soc.*, 1986, **108**, 2093–2094.
82 C. Bauer, R. Freeman, T. Frenkiel, J. Keeler and A. J. Shak, *J. Magn. Reson.*, 1984, **58**, 442–457.
83 L. Emsley and G. Bodenhausen, *J. Magn. Reson.*, 1989, **82**, 211–221.
84 A. Bax, R. H. Griffey and B. L. Hawkins, *J. Magn. Reson.*, 1983, **55**, 301–315.
85 M. El Hajji, S. Rebuffat, T. Le Doan, G. Klein, M. Satre and B. Bodo, *Biochim. Biophys. Acta*, 1989, **978**, 97–104.
86 S. C. Park, M. H. Kim, M. A. Hossain, S. Y. Shin, Y. Kim, L. Stella, J. D. Wade, Y. Park and K.-S. Hahm, *Biochim. Biophys. Acta*, 2008, **1778**, 229–241.
87 Y. Park, S. N. Park, S. C. Park, J. Y. Park, Y. H. Park, J. S. Hahm and K.-S. Hahm, *Biochem. Biophys. Res. Commun.*, 2004, **321**, 631–637.
88 M. T. Tosteson, S. J. Holmes, M. Razin and D. C. Tosteson, *J. Membrane Biol.*, 1985, **87**, 35–44.